Explicit Runge–Kutta schemes and finite elements with symmetric stabilization for first-order linear PDE systems

Erik Burman, Alexandre Ern, Miguel Angel Fernández

EXPLICIT RUNGE–KUTTA SCHEMES AND FINITE ELEMENTS WITH SYMMETRIC STABILIZATION FOR FIRST-ORDER LINEAR PDE SYSTEMS

ERIK BURMAN*, ALEXANDRE ERN†, AND MIGUEL A. FERNÁNDEZ‡

Abstract. We analyze explicit Runge–Kutta schemes in time combined with stabilized finite elements in space to approximate evolution problems with a first-order linear differential operator in space of Friedrichs-type. For the time discretization, we consider explicit second- and third-order Runge–Kutta schemes. We identify a general set of properties on the spatial stabilization, encompassing continuous and discontinuous finite elements, under which we prove stability estimates using energy arguments. Then, we establish L^2-norm error estimates with (quasi-)optimal convergence rates for smooth solutions in space and time. These results hold under the usual CFL condition for third-order Runge–Kutta schemes and any polynomial degree in space and for second-order Runge–Kutta schemes and first-order polynomials in space. For second-order Runge–Kutta schemes and higher polynomial degrees in space, a tightened 4/3-CFL condition is required. Numerical results are presented for the advection and wave equations.

Key words. First-order PDEs, transient problems, stabilized finite elements, explicit Runge–Kutta schemes, stability, convergence.

AMS subject classifications. 65M12, 65M15, 65M60, 65L06

1. Introduction. Let Ω be an open, bounded, Lipschitz domain in $\mathbb{R}^d$ and let $T > 0$ be a finite simulation time. We consider the following linear evolution problem

$$\partial_t u + Au = f \qquad \text{in } \Omega \times (0,T), \tag{1.1}$$

completed with suitable initial and boundary conditions specified below. Here, $u : \Omega \times (0,T) \to \mathbb{R}^m$, $m \geq 1$, is the unknown and $f : \Omega \times (0,T) \to \mathbb{R}^m$ is the source term. Moreover, A is a first-order linear differential operator in space endowed with a symmetry property specified below (the operator A can also accommodate a zero-order term). Typical examples include advection problems and linear wave propagation problems in electromagnetics and acoustics.

Our goal is to analyze approximations to (1.1) using explicit Runge–Kutta (RK) schemes in time and finite elements with symmetric stabilization in space. Explicit RK schemes are popular methods to approximate in time systems of ordinary differential equations. In the context of space discretization by discontinuous Galerkin (DG) methods, explicit RK schemes have been developed by Cockburn, Shu, and co-workers [11, 10, 8] and applied to a wide range of engineering problems (see, e.g., [9] and references therein). This is in stark contrast with the case of space discretization by continuous finite elements where, to our knowledge, stabilization techniques have not yet been analyzed in combination with explicit RK schemes. In particular, SUPG-type stabilization seems not to be compatible with explicit RK schemes. In fact, the only viable explicit method with continuous approximation in space for the present evolution problems is, to our knowledge, the method of characteristics [15, 25]. Alternatively, implicit methods can be considered (see, e.g., [19, 16, 7]), i.e.

*Department of Mathematics, Mantell Building, University of Sussex, Brighton, BN1 9RF United Kingdom (E.N.Burman@sussex.ac.uk)

†Université Paris-Est, CERMICS, Ecole des Ponts, 77455 Marne la Vallée Cedex 2, France (ern@cermics.enpc.fr)

‡INRIA, CRI Paris-Rocquencourt, Rocquencourt BP 105, F-78153 Le Chesnay Cedex, France (miguel.fernandez@inria.fr)

based on $\mathcal{A}$-stable time discretizations, or semi-implicit methods [7], resulting from the combination of an $\mathcal{A}$-stable scheme with an appropriate explicit treatment of the stabilization operator.

The starting point of our analysis is the observation that owing to the properties of the differential operator A, there is a real number λ_0 s.t. for the exact solution,

$$(Au, u)_L \geq \tfrac{1}{2}(Mu, u)_{L,\partial\Omega} - \lambda_0 \|u\|_L^2, \tag{1.2}$$

where M is a non-negative $\mathbb{R}^{m,m}$-valued boundary field depending on the boundary conditions. Here, we have set $L := [L^2(\Omega)]^m$, $(\cdot,\cdot)_L$ denotes the usual scalar product in L with associated norm $\|\cdot\|_L$, and $(\cdot,\cdot)_{L,\partial\Omega}$ denotes the usual scalar product in $[L^2(\partial\Omega)]^m$. As a result, an energy can be associated with the evolution problem (1.1). Indeed, taking the L-scalar product of (1.1) by u, exploiting (1.2), and integrating in time, it is inferred using Gronwall's lemma that solutions to (1.1) satisfy the energy estimate

$$\max_{t\in[0,T]} \|u\|_L^2 + \int_0^T (Mu, u)_{L,\partial\Omega} dt \leq C, \tag{1.3}$$

where the constant C depends on the initial condition, the source f, the simulation time T, and the parameter λ_0. This implies in particular that the energy, defined as the L-norm of the solution, is controlled at any time.

Following the seminal work of Levy and Tadmor [24], our analysis of explicit RK schemes with stabilized finite elements hinges on energy estimates. The crucial point is that explicit RK schemes are anti-dissipative (that is, they produce energy at each time step), and this energy production needs to be compensated by the dissipation of the stabilization scheme in space. In [24], a so-called coercivity condition was proposed on the discrete differential operator in space, and with this condition, the stability of the usual RK3 and RK4 schemes was proven under a CFL-type condition. The coercivity condition in [24] can for instance be satisfied if an artificial viscosity is used for space stabilization. However, artificial viscosity yields suboptimal convergence estimates in space as soon as finite elements with polynomials of degree ≥ 1 are used.

In the present paper, we improve on this point by establishing stability estimates for a wide class of high-order finite element methods with symmetric stabilization. High-order finite element methods do not satisfy the above coercivity condition. Instead, we derive here a sharper set of conditions on the stabilization and proceed along a different path than in [24] for the stability analysis, still relying on energy arguments. Furthermore, we additionally derive energy error estimates that are optimal in time and quasi-optimal in space provided the exact solution is smooth enough. We also consider fully unstructured simplicial meshes.

A salient feature is that our conditions allow for a unified analysis of several high-order stabilized finite element methods encountered in the literature. Examples include in the context of continuous finite elements, e.g., interior penalty of gradient jumps [2, 3], local projection [1, 26], subgrid viscosity [18, 19], or orthogonal subscale stabilization [12, 13], and also include discontinuous finite elements (DG methods) [23, 22, 17, 14]. Incidentally, a noteworthy point is that DG methods can be cast into the same unified framework as stabilized finite element methods, indicating that all these methods essentially share the same stability properties.

Explicit RK schemes come in various forms; see, e.g., [20]. Here, we present results for two-stage second-order and three-stage third-order schemes (abbreviated as RK2 and RK3, respectively). These schemes are written in a specific form suitable

for the present analysis, and we verify that usual RK2 and RK3 schemes encountered in the literature can be cast into this form.

Our main results can be summarized as follows:

- under the usual CFL condition $\tau \leq \varrho(h/\sigma)$ where τ is the time step, h the minimal mesh size, σ a reference velocity, and ϱ a dimensionless constant, an energy error estimate of the form $O(\tau^2 + h^{3/2})$ for the RK2 scheme and piecewise affine finite elements;
- under the tightened 4/3-CFL condition $\tau \leq \varrho'(h/\sigma)^{4/3}$, an energy error estimate of the form $O(\tau^2 + h^{p+1/2})$ for the RK2 scheme and finite elements with polynomials of total degree $\leq p$ with any $p \geq 2$;
- under the usual CFL condition $\tau \leq \varrho(h/\sigma)$, an energy error estimate of the form $O(\tau^3 + h^{p+1/2})$ for the RK3 scheme and finite elements with polynomials of total degree $\leq p$ with any $p \geq 1$.

To the best of our knowledge, the above results are new for continuous finite element methods. As such, they provide an attractive alternative to the method of characteristics since the present methods are more easily extendible to higher order. For DG methods, the two above results for RK2 schemes have been obtained by Zhang and Shu in the more general context of nonlinear scalar conservation laws [27] and symmetrizable systems of nonlinear conservation laws [28]. Our result for the RK3 scheme is, to the best of our knowledge, new. Moreover, the present proofs for RK2 schemes on linear PDE systems allow to identify more directly the stability properties of DG methods that play a role in the analysis.

This paper is organized as follows. In §2, we present the continuous and discrete settings and state the conditions on the stabilization of the finite element method allowing for the unified analysis. In §3 and §4, we treat RK2 and RK3 schemes, respectively. Numerical results illustrating the theory are presented in §5. Finally, some conclusions and lines for future work are drawn in §6.

2. The setting. This section presents the continuous and discrete settings together with some examples. We also state the conditions on the stabilization of the finite element method allowing for the unified analysis.

2.1. The continuous problem. Let $\{A_i\}_{1\leq i\leq d}$ be fields in $[L^\infty(\Omega)]^{m,m}$ s.t.

$$A_i \text{ is symmetric a.e. in } \Omega, \quad \forall i \in \{1,\dots,d\}, \tag{2.1}$$

$$\Lambda := \sum_{i=1}^{d} \partial_i A_i \in [L^\infty(\Omega)]^{m,m}. \tag{2.2}$$

The differential operator A in (1.1) is

$$A := \sum_{i=1}^{d} A_i \partial_i. \tag{2.3}$$

For further use, we set $\sigma := \max_{1\leq i\leq d} \|A_i\|_{[L^\infty(\Omega)]^{m,m}}$. Assuming that the PDE system (1.1) is written in non-dimensional form for u, the components of the fields A_i scale as velocities, and the quantity σ represents a maximum wave speed.

Let $n = (n_1,\dots,n_d)$ denote the outward unit normal to Ω. Define the boundary matrix field $D \in [L^\infty(\partial\Omega)]^{m,m}$ s.t. a.e. on $\partial\Omega$,

$$D := \sum_{i=1}^{d} A_i n_i, \tag{2.4}$$

and observe that D takes, by construction, symmetric values. The boundary condition on (1.1) enforces at all times $t \in (0,T)$,

$$(D-M)u|_{\partial\Omega} = 0, \tag{2.5}$$

where the boundary matrix field $M \in [L^\infty(\partial\Omega)]^{m,m}$ is non-negative a.e. on $\partial\Omega$, and $\|M\|_{[L^\infty(\partial\Omega)]^{m,m}} \leq C_M\sigma$ for some constant C_M. The initial condition is $u(\cdot,0) = u_0$ in Ω with $u_0 \in L$, and the source term is such that $f \in C^0(0,T;L)$. When deriving convergence rates, we assume that $u \in C^0(0,T;[H^{p+1}(\Omega)]^m)$ if finite elements of degree p are used, and that $u \in C^l(0,T;L)$ and $f \in C^{l-1}(0,T;L)$ with $l=3$ for RK2 and $l=4$ for RK3.

Since M is non-negative, the seminorm

$$|v|_M := (Mv,v)_{L,\partial\Omega}^{1/2}, \tag{2.6}$$

is well-defined. Define the bilinear form

$$a(v,w) = (Av,w)_L + \tfrac{1}{2}((M-D)v,w)_{L,\partial\Omega}. \tag{2.7}$$

A crucial consequence of properties (2.1) and (2.2) is that integration by parts yields

$$a(v,v) = \tfrac{1}{2}|v|_M^2 - \tfrac{1}{2}(\Lambda v,v)_L. \tag{2.8}$$

Letting $\lambda_0 := \frac{1}{2}\|\Lambda\|_{[L^\infty(\Omega)]^{m,m}}$ leads to

$$a(v,v) \geq \tfrac{1}{2}|v|_M^2 - \lambda_0\|v\|_L^2. \tag{2.9}$$

We now give three examples of evolution problems fitting the present framework.

- Advection: let $\beta \in [L^\infty(\Omega)]^d$ with $\nabla\cdot\beta \in L^\infty(\Omega)$ and consider the PDE

$$\partial_t u + \beta\cdot\nabla u = f. \tag{2.10}$$

  Set $m=1$ and

$$A_i = \beta_i,\ \forall i \in \{1,\dots,d\}, \tag{2.11}$$

  yielding $D = \beta\cdot n$. An admissible boundary condition consists in taking $M = |\beta\cdot n|$ which enforces u to zero on the inflow boundary.
- Maxwell's equations: let μ,ϵ be positive constants, set $c_0 = (\mu\epsilon)^{-1/2}$, and consider the PDE system

$$\begin{cases} \mu\partial_t H + \nabla\times E = f_1, \\ \epsilon\partial_t E - \nabla\times H = f_2, \end{cases} \tag{2.12}$$

  where H is the magnetic field and E the electric field. Set $m=6$, $u = (\mu^{1/2}H, \epsilon^{1/2}E)$, and let

$$A_i = c_0 \left[\begin{array}{c:c} 0_{3,3} & R_i \\ \hdashline R_i^t & 0_{3,3} \end{array}\right],\ \forall i \in \{1,\dots,d\}, \tag{2.13}$$

  where $0_{3,3}$ is the null matrix in $\mathbb{R}^{3,3}$ and $(R_i)_{jk} = \epsilon_{jik}$ for $i,j,k \in \{1,2,3\}$, ϵ_{jik} being the Levi–Civita permutation tensor. An admissible boundary condition

is for instance to enforce a Dirichlet condition on the tangential component of the electric field. Then, D and M are given by

$$D = c_0 \left[\begin{array}{c:c} 0_{3,3} & N \\ \hdashline N^t & 0_{3,3} \end{array}\right], \qquad M = c_0 \left[\begin{array}{c:c} 0_{3,3} & -N \\ \hdashline N^t & 0_{3,3} \end{array}\right], \tag{2.14}$$

where $N = \sum_{i=1}^3 n_i R_i \in \mathbb{R}^{3,3}$ is such that $Nz = n \times z$ for all $z \in \mathbb{R}^3$.

- Acoustics equations: let c_0 be a positive constant, and consider the PDE system

$$\left\{\begin{array}{r} c_0^{-2}\partial_t p + \nabla\cdot q = f_1, \\ \partial_t q + \nabla p = f_2, \end{array}\right. \tag{2.15}$$

where p is the pressure and q the momentum per unit volume. Set $m = 4$, $u = (c_0^{-1}p, q)$, and let

$$A_i = c_0 \left[\begin{array}{c:c} 0 & e_i^t \\ \hdashline e_i & 0_{3,3} \end{array}\right], \ \forall i \in \{1, \ldots, d\}, \tag{2.16}$$

where (e_1, e_2, e_3) denotes the Cartesian basis of $\mathbb{R}^3$. An admissible boundary condition is for instance to enforce a Dirichlet condition on the normal component of the flux. Then, D and M are given by

$$D = c_0 \left[\begin{array}{c:c} 0 & n^t \\ \hdashline n & 0_{3,3} \end{array}\right], \qquad M = c_0 \left[\begin{array}{c:c} 0 & -n^t \\ \hdashline n & 0_{3,3} \end{array}\right]. \tag{2.17}$$

2.2. Space discretization. Let $\{\mathcal{T}_h\}_{h>0}$ be a family of simplicial meshes of Ω where h denotes the maximum diameter of elements in $\mathcal{T}_h$. For simplicity, we assume that the meshes are affine. Mesh faces are collected in the set $\mathcal{F}_h$ which is split into the set of interior faces, $\mathcal{F}_h^{\rm int}$, and boundary faces, $\mathcal{F}_h^{\rm ext}$. For $T \in \mathcal{T}_h$ and for $F \in \mathcal{F}_h$, $\|\cdot\|_{L,T}$ and $\|\cdot\|_{L,F}$ respectively denote the $[L^2(T)]^m$- and $[L^2(F)]^m$-norms; moreover, we define $\|\cdot\|_{L,\mathcal{F}_h}^2 := \sum_{F\in\mathcal{F}_h} \|\cdot\|_{L,F}^2$. We assume that meshes are kept fixed in time and also that the family $\{\mathcal{T}_h\}_{h>0}$ is quasi-uniform; see Remark 2.1 below.

Let V_h be a finite element space consisting of either continuous or discontinuous piecewise polynomials of total degree $\le p$ with $p \ge 1$ (the case $p = 0$ is also possible for DG methods). Let π_h denote the L-orthogonal projection onto V_h. Set $V(h) := [H^{p+1}(\Omega)]^m + V_h$. We consider a discrete version of the bilinear form a, namely a_h, together with a stabilization bilinear form s_h. Both forms are defined on $V(h) \times V_h$. We define the linear operators $A_h : V(h) \to V_h$ and $S_h : V(h) \to V_h$ s.t. $\forall (v, w_h) \in V(h) \times V_h$,

$$(A_h v, w_h)_L := a_h(v, w_h), \qquad (S_h v, w_h)_L := s_h(v, w_h). \tag{2.18}$$

We also define $L_h : V(h) \to V_h$ s.t.

$$L_h = A_h + S_h. \tag{2.19}$$

The seminorm $|\cdot|_M$ defined above can be extended to $V(h)$.

We now state the key design conditions on the bilinear forms a_h and s_h. The first three assumptions are the following:

(A1) for all $v_h \in V_h$, $a_h(v_h, v_h) = \frac{1}{2}|v_h|_M^2 - \frac{1}{2}(\Lambda v_h, v_h)_L$;
(A2) s_h is symmetric and non-negative on $V(h) \times V_h$;
(A3) the strong solution u satisfies for all $t \in (0,T)$, $L_h u = \pi_h(f - \partial_t u)$.

Assumption **(A3)** is a (strong) consistency property; it is equivalent to the fact that for the strong solution u, for all $t \in (0,T)$, and for all $v_h \in V_h$,

$$a_h(u, v_h) + s_h(u, v_h) = a(u, v_h). \tag{2.20}$$

This consistency property can be weakened for the stabilization bilinear form s_h. This is, in particular, useful when analyzing local projection or orthogonal subscale stabilization. The present strong consistency assumption is sufficient to analyze interior penalty stabilization and DG methods; see Section 2.4 for examples. Furthermore, owing to Assumption **(A2)**, we can define on $V(h)$ the seminorm

$$|v|_S := \left\{ s_h(v,v) + \tfrac{1}{2}|v|_M^2 \right\}^{1/2}. \tag{2.21}$$

The other assumptions concern the stability of the discrete operators S_h and L_h, namely

(A4) there is C_S s.t. for all $v_h \in V_h$,

$$|v_h|_S \le C_S^{1/2} \sigma^{1/2} h^{-1/2} \|v_h\|_L, \tag{2.22}$$

and there is C_S' s.t. for all $v \in [H^{p+1}(\Omega)]^m$,

$$|v - \pi_h v|_S \le C_S' h^{p+1/2} \|v\|_{[H^{p+1}(\Omega)]^m}; \tag{2.23}$$

(A5) there is C_L s.t. for all $z \in V(h)$,

$$\|L_h z\|_L \le C_L(\sigma \|\nabla_h z\|_{L^d} + \sigma^{1/2} h^{-1/2} |z|_S), \tag{2.24}$$

where ∇_h denotes the broken gradient of z and $\|\cdot\|_{L^d}$ the usual norm in L^d (the broken gradient is needed when working with DG methods; it coincides with the usual gradient for continuous finite elements);

(A6) there is C_π s.t. for all $(z, v_h) \in V(h) \times V_h$,

$$|(L_h(z - \pi_h z), v_h)_L| \le C_\pi \sigma^{1/2} \|z - \pi_h z\|_* (|v_h|_S + \|v_h\|_L), \tag{2.25}$$

with the norm for $y \in V(h)$,

$$\|y\|_* := h^{1/2} \|\nabla_h y\|_{L^d} + h^{-1/2} \|y\|_L + \|y\|_{L,\mathcal{F}_h} + \sigma^{-1/2} |y|_S. \tag{2.26}$$

Finally, in the piecewise affine case, that is, $p = 1$ in the definition of the discrete space V_h, we also assume that

(A7) there is C_π' s.t. for all $(v_h, w_h) \in V_h \times V_h$ with $p = 1$,

$$|(L_h v_h, w_h - \pi_h^0 w_h)_L| \le C_\pi' \sigma^{1/2} h^{-1/2} (|v_h|_S + \|v_h\|_L) \|w_h - \pi_h^0 w_h\|_L, \tag{2.27}$$

where π_h^0 denotes the L-orthogonal projection onto piecewise constant functions.

Our analysis hinges on Assumptions **(A1)**–**(A7)**. For further use, we point out some useful facts associated with these assumptions. An important consequence of **(A1)**–**(A2)** and the definition (2.21) of the seminorm $|\cdot|_S$ is the following dissipativity property of the discrete setting: For all $v_h \in V_h$,

$$(L_h v_h, v_h)_L = |v_h|_S^2 - \tfrac{1}{2}(\Lambda v_h, v_h)_L. \tag{2.28}$$

Moreover, it is clear that **(A5)** implies for all $z \in V(h)$,

$$\|L_h z\|_L \le C_L \sigma h^{-1/2} \|z\|_*. \tag{2.29}$$

Using inverse and trace inequalities, it is readily inferred from the definition (2.26) of the norm $\|\cdot\|_*$ that there is C_* such that for all $v_h \in V_h$,

$$\|v_h\|_* \le C_* h^{-1/2} \|v_h\|_L. \tag{2.30}$$

Hence, letting $C_{L*} := C_L C_*$, there holds for all $v_h \in V_h$,

$$\|L_h v_h\|_L \le C_{L*} \sigma h^{-1} \|v_h\|_L. \tag{2.31}$$

Finally, using (2.23) and usual approximation properties in finite element spaces, it is inferred that there is C'_* s.t. for all $v \in [H^{p+1}(\Omega)]^m$,

$$\|v - \pi_h v\|_* \le C'_* h^{p+1/2} \|v\|_{[H^{p+1}(\Omega)]^m}. \tag{2.32}$$

2.3. CFL conditions. Let τ be the time step, taken to be constant for simplicity and such that $T = N\tau$ where N is an integer. For $0 \le n \le N$, a superscript n indicates the value of a function at the discrete time $n\tau$, and for $0 \le n \le N-1$, we set $I_n = [n\tau, (n+1)\tau]$. We assume without loss of generality that $\tau \le 1$. We also assume that the following, so-called usual, CFL condition holds

$$\tau \le \varrho(h/\sigma), \tag{2.33}$$

for some positive real number ϱ. The value of ϱ will be specified below whenever relevant. Furthermore, in the case of RK2 schemes with polynomials of total degree ≥ 2, we will also need the so-called strengthened 4/3-CFL condition

$$\tau \le \varrho'(h/\sigma)^{4/3}, \tag{2.34}$$

for some positive real number ϱ'. Again, the value of ϱ' will be specified below whenever relevant. Since $\tau \le 1$, the strengthened 4/3-CFL condition (2.34) implies the CFL condition (2.33) with $\varrho = (\varrho')^{3/4}$.

REMARK 2.1. *It is also possible to work with shape-regular mesh families. In this case, as usual, the space scale in the CFL condition is no longer h, but the smallest element diameter in the mesh. The same space scale is used in the negative powers of h in Assumptions **(A4)**–**(A7)**.*

2.4. Examples. In this section, we present two examples of discrete bilinear forms satisfying Assumptions **(A1)**–**(A7)**. For $F \in \mathcal{F}_h^{\rm int}$, there are T^-, T^+ in $\mathcal{T}_h$ such that $F = \partial T^- \cap \partial T^+$, n_F is the unit normal to F pointing from T^- to T^+, and for a smooth enough function v that is possibly double-valued at F, we define its jump and mean value at F as $[\![v]\!] := v|_{T^-} - v|_{T^+}$ and $\{\!\{v\}\!\} = \frac{1}{2}(v|_{T^-} + v|_{T^+})$, respectively. For vector-valued functions, the jump and averages are defined componentwise as above. The arbitrariness in the sign of $[\![v]\!]$ is irrelevant. Meshes can possess hanging nodes when working with discontinuous finite elements.

An example with continuous finite elements consists in considering symmetric stabilization based on inter-element jumps of the gradient of the discrete solution [2, 3, 5]. In this case,

$$a_h^{\rm cip}(v,w) := \sum_{T\in\mathcal{T}_h} (Av, w)_{L,T} + \sum_{F\in\mathcal{F}_h^{\rm ext}} \tfrac{1}{2}((M-D)v, w)_{L,F}, \tag{2.35}$$

$$s_h^{\rm cip}(v,w) := \sum_{F\in\mathcal{F}_h^{\rm ext}} (S_F^{\rm ext} v, w)_{L,F} + \sum_{F\in\mathcal{F}_h^{\rm int}} h_F^2 (S_F^{\rm int} n_F \cdot [\![\nabla v]\!], n_F \cdot [\![\nabla w]\!])_{L,F}, \tag{2.36}$$

where h_F denotes the diameter of F. An example with discontinuous finite elements consists in taking [17]

$$a_h^{\rm dg}(v,w) := a^{\rm cip}(v,w) - \sum_{F\in\mathcal{F}_h^{\rm int}} (D_F[\![v]\!], \{\!\{w\}\!\})_{L,F}, \tag{2.37}$$

$$s_h^{\rm dg}(v,w) := \sum_{F\in\mathcal{F}_h^{\rm ext}} (S_F^{\rm ext} v, w)_{L,F} + \sum_{F\in\mathcal{F}_h^{\rm int}} (S_F^{\rm int}[\![v]\!], [\![w]\!])_{L,F}, \tag{2.38}$$

where $D_F := \sum_{i=1}^d A_i n_{F,i}$ for all $F \in \mathcal{F}_h^{\rm int}$.

The $\mathbb{R}^{m,m}$-valued fields $S_F^{\rm ext}$ and $S_F^{\rm int}$, which are defined on boundary and interior faces, respectively, must satisfy the following design conditions:

$$\text{for the exact solution } u \text{ and for all } t\in[0,T],\ S_F^{\rm ext} u = 0 \text{ on } \partial\Omega, \tag{2.39}$$

$$S_F^{\rm ext} \text{ and } S_F^{\rm int} \text{ are symmetric and non-negative,} \tag{2.40}$$

$$\forall F\in\mathcal{F}_h^{\rm ext},\ S_F^{\rm ext} \le \alpha_1\sigma I_m \quad\text{and}\quad \forall F\in\mathcal{F}_h^{\rm int},\ \alpha_2|D_F| \le S_F^{\rm int} \le \alpha_3\sigma I_m, \tag{2.41}$$

and for all $F\in\mathcal{F}_h^{\rm ext}$ and for all $(y,z)\in[L^2(F)]^m\times[L^2(F)]^m$,

$$|((M-D)y,z)_{L,F}| \le \alpha_4\sigma^{1/2}|y|_{S,F}\|z\|_{L,F}, \tag{2.42}$$

$$|((M+D)y,z)_{L,F}| \le \alpha_5\sigma^{1/2}\|y\|_{L,F}|z|_{S,F}. \tag{2.43}$$

Here, $\alpha_1,\dots,\alpha_5$ are positive parameters, inequalities in (2.41) are meant on the associated quadratic forms, I_m denotes the identity matrix in $\mathbb{R}^{m,m}$, and for $F\in\mathcal{F}_h^{\rm ext}$, $|v|_{S,F} := \{(S_F^{\rm ext}v,v)_{L,F} + (Mv,v)_{L,F}\}^{1/2}$ which is well-defined since $S_F^{\rm ext}$ is non-negative. The absolute value $|D_F|$ is also well-defined since D_F is, by construction, symmetric.

LEMMA 2.1. *Assume that the design conditions* (2.39)–(2.43) *hold and that for all* $T\in\mathcal{T}_h$ *and for all* $i\in\{1,\dots,d\}$, $A_i|_T \in [C^{0,1/2}(T)]^{m,m}$. *Then, Assumptions* ***(A1)***–***(A7)*** *hold for* $a_h^{\rm cip}$ *and* $s_h^{\rm cip}$ *defined by* (2.35)–(2.36) *and for* $a_h^{\rm dg}$ *and* $s_h^{\rm dg}$ *defined by* (2.37)–(2.38).

Proof. Assumptions **(A1)**–**(A6)** can be proven as in [5, 6] for continuous finite elements with interior penalty and as in [17] for discontinuous finite elements. To prove Assumption **(A7)** for continuous finite elements, let $(v_h,w_h)\in V_h\times V_h$ with $p=1$ and set $y_h = w_h - \pi_h^0 w_h$. Since y_h may not be in V_h, we obtain

$$(L_h v_h, y_h)_L = \sum_{T\in\mathcal{T}_h} (Av_h, \pi_h y_h)_{L,T} + \sum_{F\in\mathcal{F}_h^{\rm ext}} \tfrac12((M-D)v_h,\pi_h y_h)_{L,F} + s_h^{\rm cip}(v_h,\pi_h y_h).$$

For the third term, using **(A2)** and **(A4)** we obtain

$$\begin{aligned}|s_h^{\rm cip}(v_h,\pi_h y_h)| \le |v_h|_S|\pi_h y_h|_S &\le |v_h|_S C_S^{1/2}\sigma^{1/2}h^{-1/2}\|\pi_h y_h\|_L\\ &\le C_S^{1/2}\sigma^{1/2}h^{-1/2}|v_h|_S\|y_h\|_L.\end{aligned}$$

The second term is bounded similarly using (2.42) and a trace inequality to bound $\|\pi_h y_h\|_{L,F}$. For the first term, observe that

$$\sum_{T\in\mathcal{T}_h} (Av_h,\pi_h y_h)_{L,T} = \sum_{T\in\mathcal{T}_h} (Av_h,\pi_h y_h - y_h)_{L,T} + \sum_{T\in\mathcal{T}_h} (Av_h,y_h)_{L,T} := T_1 + T_2.$$

Following [5] using a so-called Oswald interpolate, it can be proven that

$$|T_1| \le C\sigma^{1/2}h^{-1/2}(|v_h|_S + \|v_h\|_L)\|y_h\|_L.$$

Furthermore, since $p = 1$, letting $\overline{A} := \sum_{i=1}^{d}(\pi_h^0 A_i)\partial_i$,

$$T_2 = \sum_{T\in\mathcal{T}_h}((A-\overline{A})v_h, y_h)_{L,T} \le C\sigma^{1/2}h^{-1/2}\|v_h\|_L\|y_h\|_L,$$

using the local regularity of the fields A_i and an inverse inequality. This completes the proof of Assumption **(A7)** for continuous finite elements. For discontinuous finite elements, the proof is similar, but simpler since $\pi_h y_h = y_h$ and so $T_1 = 0$. □

The above setting can be applied to the PDE systems presented in §2.1; see [5, 17].

- Advection: take $S_F^{\rm ext} = 0$ and $S_F^{\rm int} = \gamma|\beta{\cdot}n_F|$ with user-defined parameter $\gamma > 0$ ($\gamma = \frac{1}{2}$ amounts to so-called upwinding in the context of DG methods).
- Maxwell's equations: take

$$S_F^{\rm ext} = c_0\left[\begin{array}{c|c} 0_{3,3} & 0_{3,3} \\ \hline 0_{3,3} & \gamma_1 N^t N \end{array}\right], \qquad S_F^{\rm int} = c_0\left[\begin{array}{c|c} \gamma_2 N_F^t N_F & 0_{3,3} \\ \hline 0_{3,3} & \gamma_3 N_F^t N_F \end{array}\right], \tag{2.44}$$

  where γ_1, γ_2, and γ_3 are positive user-defined parameters and where N_F is defined as N by using n_F instead of n. The operator $S_F^{\rm int}$ amounts to penalizing on each interface the jump of the normal derivative (for CIP) or of the value (for DG) of the tangential components of the electric and magnetic fields.
- Acoustics: take

$$S_F^{\rm ext} = c_0\left[\begin{array}{c|c} 0 & 0_3^t \\ \hline 0_3 & \gamma_1 n\otimes n \end{array}\right], \qquad S_F^{\rm int} = c_0\left[\begin{array}{c|c} \gamma_2 & 0_3^t \\ \hline 0_3 & \gamma_3 n_F\otimes n_F \end{array}\right], \tag{2.45}$$

  where 0_3 is the null vector in $\mathbb{R}^3$. The operator $S_F^{\rm int}$ amounts to penalizing on each interface the jump of the normal derivative (for CIP) or of the value (for DG) of the pressure and that of the normal component of the momentum per unit volume.

3. Analysis for explicit RK2 schemes. This section is devoted to the convergence analysis of explicit two-stage RK2 schemes. First, we present the specific form of the schemes on which we will work and show that usual implementations of two-stage RK2 schemes fit this form. Then, we derive the error equation and establish the key energy identity. Finally, we infer (quasi-)optimally convergent error upper bounds under the CFL condition (2.33) for piecewise affine finite elements and under the strengthened 4/3-CFL condition (2.34) for polynomials with total degree ≥ 2. We will keep track of the constants to derive the CFL conditions, but not to state the error estimates. Henceforth, C denotes a generic constant, independent of the mesh size and the time step, but that can depend on f, u, the fields A_i and M, the constants in Assumptions **(A4)**–**(A7)**, and the constants ϱ and ϱ' in the CFL condition, and whose value can change at each occurrence. The inequality $a \le Cb$, for positive real numbers a and b, is often abbreviated as $a \lesssim b$. This convention is kept for the rest of this work. We also set $f_h := \pi_h f$. Finally, recall that we assume here $u \in C^3(0,T;L)$ and $f \in C^2(0,T;L)$.

3.1. Two-stage RK2 schemes. We consider schemes of the form

$$w_h^n = u_h^n - \tau L_h u_h^n + \tau f_h^n, \tag{3.1}$$
$$u_h^{n+1} = \tfrac{1}{2}(u_h^n + w_h^n) - \tfrac{1}{2}\tau L_h w_h^n + \tfrac{1}{2}\tau \psi_h^n, \tag{3.2}$$

with the assumption that

$$\psi_h^n = f_h^n + \tau \partial_t f_h^n + \delta_h^n, \qquad \|\delta_h^n\|_L \lesssim \tau^2. \tag{3.3}$$

There are many ways of writing explicit two-stage RK2 schemes. Since the space differential operator is linear, they all amount in the homogeneous case ($f = 0$) to

$$u_h^{n+1} = u_h^n - \tau L_h u_h^n + \tfrac{1}{2}\tau^2 L_h^2 u_h^n. \tag{3.4}$$

Two examples of two-stage RK2 schemes that fit the present form are:

- The second-order Heun method which is usually written in the form (3.1)–(3.2) with

$$\psi_h^n = f_h^{n+1}. \tag{3.5}$$

  Assumption (3.3) obviously holds.
- The second-order Runge method (also called the improved forward Euler method) which is usually written in the form

$$k_1 = -L_h u_h^n + f_h^n, \tag{3.6}$$
$$k_2 = -L_h(u_h^n + \tfrac{1}{2}\tau k_1) + f_h^{n+1/2}, \tag{3.7}$$
$$u_h^{n+1} = u_h^n + \tau k_2. \tag{3.8}$$

  It is readily verified that (3.6)–(3.8) can be rewritten in the form (3.1)–(3.2) with

$$\psi_h^n = 2 f_h^{n+1/2} - f_h^n. \tag{3.9}$$

  Assumption (3.3) obviously holds.

Define

$$\xi_h^n = u_h^n - \pi_h u^n, \qquad \zeta_h^n = w_h^n - \pi_h w^n, \tag{3.10}$$
$$\xi_\pi^n = u^n - \pi_h u^n, \qquad \zeta_\pi^n = w^n - \pi_h w^n, \tag{3.11}$$

with $w = u + \tau \partial_t u$. Using these quantities, the errors can be written as

$$u^n - u_h^n = \xi_\pi^n - \xi_h^n, \qquad w^n - w_h^n = \zeta_\pi^n - \zeta_h^n. \tag{3.12}$$

The convergence analysis proceeds as follows. Since upper bounds on ξ_π^n and ζ_π^n readily result from standard approximation properties in finite element spaces, we observe that error upper bounds can be derived by obtaining upper bounds on ξ_h^n and ζ_h^n in terms of ξ_π^n and ζ_π^n and then using the triangle inequality. To this purpose, we first identify the error equation governing the time evolution of ξ_h^n and ζ_h^n. The form of this equation is similar to (3.1)–(3.2) with data depending on ξ_π^n, ζ_π^n, f, and u. Then, we establish an energy identity associated with (3.1)–(3.2), whence the desired upper bounds on ξ_h^n and ζ_h^n are inferred.

3.2. The error equation. Our first lemma identifies the equations governing the quantities ξ_h^n and ζ_h^n.

LEMMA 3.1. *There holds*

$$\zeta_h^n = \xi_h^n - \tau L_h \xi_h^n + \tau \alpha_h^n, \tag{3.13}$$

$$\xi_h^{n+1} = \tfrac{1}{2}(\xi_h^n + \zeta_h^n) - \tfrac{1}{2}\tau L_h \zeta_h^n + \tfrac{1}{2}\tau \beta_h^n, \tag{3.14}$$

with

$$\alpha_h^n = L_h \xi_\pi^n, \qquad \beta_h^n = L_h \zeta_\pi^n - \pi_h \eta^n + \delta_h^n, \tag{3.15}$$

with $\eta^n = \tau^{-1} \int_{I_n} (t_{n+1} - t)^2 \partial_{ttt} u \, dt$.

Proof. Recalling Assumption **(A3)**, namely $\pi_h \partial_t u^n = -L_h u^n + f_h^n$, yields

$$\pi_h w^n = \pi_h u^n - \tau L_h u^n + \tau f_h^n.$$

Subtracting this equation from (3.1) yields (3.13). To derive (3.14), observe that

$$u^{n+1} = u^n + \tau \partial_t u^n + \tfrac{1}{2}\tau^2 \partial_{tt} u^n + \tfrac{1}{2}\tau \eta^n,$$

and projecting yields

$$\begin{aligned} \pi_h u^{n+1} &= \pi_h w^n + \tfrac{1}{2}\tau^2 \pi_h \partial_{tt} u^n + \tfrac{1}{2}\tau \pi_h \eta^n \\ &= \tfrac{1}{2}(\pi_h u^n + \pi_h w^n) - \tfrac{1}{2}\tau L_h u^n + \tfrac{1}{2}\tau f_h^n + \tfrac{1}{2}\tau^2 \pi_h \partial_{tt} u^n + \tfrac{1}{2}\tau \pi_h \eta^n. \end{aligned}$$

Moreover,

$$\tau \pi_h \partial_{tt} u^n = \tau \partial_t (\pi_h \partial_t u^n) = -\tau L_h \partial_t u^n + \tau \partial_t f_h^n = -L_h (w^n - u^n) + \tau \partial_t f_h^n,$$

whence

$$\pi_h u^{n+1} = \tfrac{1}{2}(\pi_h u^n + \pi_h w^n) - \tfrac{1}{2}\tau L_h w^n + \tfrac{1}{2}\tau (\pi_h \eta^n + f_h^n + \tau \partial_t f_h^n).$$

Subtracting this equation from (3.2) yields (3.14). ∎

For further use, it is convenient to observe that (3.13)–(3.14) imply

$$\xi_h^{n+1} = \zeta_h^n - \tfrac{1}{2}\tau L_h (\zeta_h^n - \xi_h^n) + \tfrac{1}{2}\tau (\beta_h^n - \alpha_h^n). \tag{3.16}$$

3.3. Energy identity and stability. Our next step is to derive an energy identity, then leading to our main stability estimate.

LEMMA 3.2 (Energy identity). *There holds*

$$\begin{aligned} \|\xi_h^{n+1}\|_L^2 - \|\xi_h^n\|_L^2 + \tau |\xi_h^n|_S^2 + \tau |\zeta_h^n|_S^2 &= \|\xi_h^{n+1} - \zeta_h^n\|_L^2 \\ &+ \tau (\alpha_h^n, \xi_h^n)_L + \tau (\beta_h^n, \zeta_h^n)_L + \tfrac{1}{2}\tau (\Lambda \xi_h^n, \xi_h^n)_L + \tfrac{1}{2}\tau (\Lambda \zeta_h^n, \zeta_h^n)_L. \end{aligned} \tag{3.17}$$

Proof. Multiply (3.13) by ξ_h^n and (3.14) by $2\zeta_h^n$, sum both equations, and use (2.28) to infer $(L_h \xi_h^n, \xi_h^n)_L = |\xi_h^n|_S^2 - \tfrac{1}{2}(\Lambda \xi_h^n, \xi_h^n)_L$ and $(L_h \zeta_h^n, \zeta_h^n)_L = |\zeta_h^n|_S^2 - \tfrac{1}{2}(\Lambda \zeta_h^n, \zeta_h^n)_L$. ∎

REMARK 3.1. *The quantity* $\|\xi_h^{n+1} - \zeta_h^n\|_L^2$ *appearing in the right-hand side of the energy identity* (3.17) *is the anti-dissipative term associated with the explicit nature of the RK2 scheme. This term essentially amounts to a second-order derivative in time.*

LEMMA 3.3 (Stability). *Under the usual CFL condition* (2.33) *for any positive real number* ϱ*, there holds*

$$\|\xi_h^{n+1}\|_L^2 - \|\xi_h^n\|_L^2 + \tfrac{1}{2}\tau|\xi_h^n|_S^2 + \tfrac{1}{2}\tau|\zeta_h^n|_S^2 \le \|\xi_h^{n+1} - \zeta_h^n\|_L^2 + C\tau(\tau^4 + \|\xi_\pi^n\|_*^2 + \|\zeta_\pi^n\|_*^2 + \|\xi_h^n\|_L^2). \quad (3.18)$$

Proof. Starting with the energy identity (3.17), we bound the last four terms in the right-hand side.
(i) We first bound α_h^n and β_h^n. Let us prove that

$$\tau\|\alpha_h^n\|_L \lesssim \tau^{1/2}\|\xi_\pi^n\|_*, \qquad \tau\|\beta_h^n\|_L \lesssim \tau^{1/2}\|\zeta_\pi^n\|_* + \tau^3, \quad (3.19)$$

and that for all $v_h \in V_h$,

$$\tau(\alpha_h^n, v_h)_L \lesssim \tau\|\xi_\pi^n\|_*(|v_h|_S + \|v_h\|_L), \quad (3.20)$$
$$\tau(\beta_h^n, v_h)_L \lesssim \tau\|\zeta_\pi^n\|_*(|v_h|_S + \|v_h\|_L) + \tau^3\|v_h\|_L. \quad (3.21)$$

Using the definition of α_h^n, the bound (2.29), and the CFL condition (2.33) to eliminate the factor $h^{-1/2}$ yields

$$\tau\|\alpha_h^n\|_L = \tau\|L_h\xi_\pi^n\|_L \le \tau C_L\sigma h^{-1/2}\|\xi_\pi^n\|_* \lesssim \tau^{1/2}\|\xi_\pi^n\|_*.$$

Similarly, using the definition of β_h^n, the assumption on δ_h^n, and the regularity of the strong solution u yields

$$\tau\|\beta_h^n\|_L = \tau\|L_h\zeta_\pi^n - \pi_h\eta^n + \delta_h^n\|_L \lesssim \tau\|L_h\zeta_\pi^n\|_L + \tau^3 \lesssim \tau^{1/2}\|\zeta_\pi^n\|_* + \tau^3.$$

This proves (3.19). In addition, owing to Assumption **(A6)**,

$$\tau(\alpha_h^n, v_h)_L = \tau(L_h\xi_\pi^n, v_h)_L \lesssim \tau\|\xi_\pi^n\|_*(|v_h|_S + \|v_h\|_L),$$

and similarly, using a Cauchy–Schwarz inequality,

$$\tau(\beta_h^n, v_h)_L = \tau(L_h\zeta_\pi^n, v_h)_L + \tau(-\pi_h\eta^n + \delta_h^n, v_h)_L \lesssim \tau\|\zeta_\pi^n\|_*(|v_h|_S + \|v_h\|_L) + \tau^3\|v_h\|_L.$$

(ii) Owing to the bounds (3.20) and (3.21),

$$\tau(\alpha_h^n, \xi_h^n)_L + \tau(\beta_h^n, \zeta_h^n)_L \lesssim \tau\|\xi_\pi^n\|_*(|\xi_h^n|_S + \|\xi_h^n\|_L) + \tau\|\zeta_\pi^n\|_*(|\zeta_h^n|_S + \|\zeta_h^n\|_L) + \tau^3\|\zeta_h^n\|_L.$$

Moreover, it is inferred from (3.13) using the triangle inequality, the bound (2.31), and the CFL condition (2.33) that

$$\|\zeta_h^n\|_L \le \|\xi_h^n\|_L + \tau\|L_h\xi_h^n\|_L + \tau\|\alpha_h^n\|_L \lesssim \|\xi_h^n\|_L + \tau\|\alpha_h^n\|_L.$$

Hence, owing to (3.19),

$$\|\zeta_h^n\|_L \lesssim \|\xi_h^n\|_L + \tau^{1/2}\|\xi_\pi^n\|_* \le \|\xi_h^n\|_L + \|\xi_\pi^n\|_*,$$

since $\tau \le 1$. Collecting these bounds and using Young inequalities yields

$$\tau(\alpha_h^n, \xi_h^n)_L + \tau(\beta_h^n, \zeta_h^n)_L \le \tfrac{1}{2}\tau|\xi_h^n|_S^2 + \tfrac{1}{2}\tau|\zeta_h^n|_S^2 + C\tau(\tau^4 + \|\xi_\pi^n\|_*^2 + \|\zeta_\pi^n\|_*^2 + \|\xi_h^n\|_L^2).$$

(iii) Finally,

$$\tfrac{1}{2}\tau(\Lambda\xi_h^n, \xi_h^n)_L + \tfrac{1}{2}\tau(\Lambda\zeta_h^n, \zeta_h^n)_L \lesssim \tau\|\xi_h^n\|_L^2 + \tau\|\zeta_h^n\|_L^2 \lesssim \tau\|\xi_h^n\|_L^2 + \tau\|\xi_\pi^n\|_*^2,$$

since $\|\zeta_h^n\|_L \lesssim \|\xi_h^n\|_L + \|\xi_\pi^n\|_*$. This concludes the proof. ∎

3.4. Error estimates. Starting from the stability estimate (3.18), there are two ways to bound the positive term $\|\xi_h^{n+1} - \zeta_h^n\|_L^2$ appearing in the right-hand side. In the general case $p \geq 2$, the strengthened 4/3-CFL condition (2.34) is needed. By proceeding differently and using Assumption **(A7)** for $p = 1$, it is possible to control this term using only the usual CFL condition (2.33).

3.4.1. General case: 4/3-CFL condition. The next theorem provides a general *a priori* error estimate in the general case $p \geq 2$ under the strengthened 4/3-CFL condition.

THEOREM 3.1. *Assume that* $u \in C^3(0,T;L) \cap C^0(0,T;[H^{p+1}(\Omega)]^m)$. *Under the strengthened* 4/3*-CFL condition* (2.34) *for any positive real number* ϱ', *there holds*

$$\|u^N - u_h^N\|_L + \left(\sum_{n=0}^{N-1} \tfrac{1}{2}\tau|u_h^n|_S^2 + \tfrac{1}{2}\tau|w_h^n|_S^2\right)^{1/2} \lesssim \tau^2 + h^{p+1/2}. \tag{3.22}$$

Proof. The proof is decomposed into three steps.
(i) Bound on $\|\xi_h^{n+1} - \zeta_h^n\|_L^2$. Starting from (3.16) and using (3.13) leads to

$$\begin{aligned}\xi_h^{n+1} - \zeta_h^n &= -\tfrac{1}{2}\tau L_h(\zeta_h^n - \xi_h^n) + \tfrac{1}{2}\tau(\beta_h^n - \alpha_h^n)\\ &= \tfrac{1}{2}\tau^2 L_h^2 \xi_h^n + \tfrac{1}{2}\tau(\beta_h^n - \alpha_h^n - \tau L_h \alpha_h^n).\end{aligned}$$

Set $R_h^n = \frac{1}{2}\tau(\beta_h^n - \alpha_h^n - \tau L_h \alpha_h^n)$. Using the triangle inequality, the bound (2.31), and the CFL condition (2.33) yields

$$\|R_h^n\|_L \lesssim \tau\|\beta_h^n\|_L + \tau\|\alpha_h^n\|_L,$$

so that (3.19) implies

$$\|R_h^n\|_L \lesssim \tau^3 + \tau^{1/2}\|\zeta_\pi^n\|_* + \tau^{1/2}\|\xi_\pi^n\|_*.$$

As a result,

$$\|\xi_h^{n+1} - \zeta_h^n\|_L^2 \lesssim \tau^4\|L_h^2\xi_h^n\|_L^2 + \tau(\tau^5 + \|\xi_\pi^n\|_*^2 + \|\zeta_\pi^n\|_*^2).$$

(ii) Using the above bound together with the stability estimate (3.18) leads to

$$\|\xi_h^{n+1}\|_L^2 - \|\xi_h^n\|_L^2 + \tfrac{1}{2}\tau|\xi_h^n|_S^2 + \tfrac{1}{2}\tau|\zeta_h^n|_S^2 \lesssim \tau^4\|L_h^2\xi_h^n\|_L^2 + \tau(\tau^4 + \|\xi_\pi^n\|_*^2 + \|\zeta_\pi^n\|_*^2 + \|\xi_h^n\|_L^2),$$

since $\tau^5 \leq \tau^4$. The strengthened 4/3-CFL condition together with (2.31) imply

$$\tau^4\|L_h^2\xi_h^n\|_L^2 \lesssim \tau\|\xi_h^n\|_L^2.$$

Hence,

$$\|\xi_h^{n+1}\|_L^2 - \|\xi_h^n\|_L^2 + \tfrac{1}{2}\tau|\xi_h^n|_S^2 + \tfrac{1}{2}\tau|\zeta_h^n|_S^2 \lesssim \tau\|\xi_h^n\|_L^2 + \tau(\tau^4 + \|\xi_\pi^n\|_*^2 + \|\zeta_\pi^n\|_*^2).$$

(iii) Summing over n in the above estimate and using Gronwall's lemma, it is inferred that

$$\|\xi_h^N\|_L^2 + \sum_{n=0}^{N-1} \tfrac{1}{2}\tau(|\xi_h^n|_S^2 + |\zeta_h^n|_S^2) \lesssim \tau^4 + \sum_{n=0}^{N-1} \tau(\|\xi_\pi^n\|_*^2 + \|\zeta_\pi^n\|_*^2),$$

and using the approximation property (2.32) yields

$$\|\xi_h^N\|_L^2 + \sum_{n=0}^{N-1} \tfrac{1}{2}\tau(|\xi_h^n|_S^2 + |\zeta_h^n|_S^2) \lesssim \tau^4 + h^{2p+1},$$

whence (3.22) readily follows using a triangle inequality and the fact that $|u - u_h^n|_S = |u_h^n|_S$ and $|w - w_h^n|_S = |w_h^n|_S$. ∎

REMARK 3.2. *Although there is no specific limit to the value of the constant ϱ' in the 4/3-CFL condition for the convergence result of Theorem 3.1 to hold, the constant in the error estimate depends exponentially on ϱ'. Hence, in practice, a small enough value should be considered for ϱ'; see Section 5 for numerical experiments.*

3.4.2. Piecewise affine finite elements: usual CFL condition. The next theorem provides an *a priori* error estimate for $p = 1$ under the usual CFL condition.

THEOREM 3.2. *Assume piecewise affine finite elements are used and that $u \in C^3(0,T;L) \cap C^0(0,T;[H^2(\Omega)]^m)$. Then, under the usual CFL condition* (2.33) *with*

$$\varrho \le \min\left\{(2\sqrt{2}C_L)^{-2}, (2\sqrt{2}C_L C_i')^{-2/3}\right\}, \tag{3.23}$$

with $C_i' = C_i C_\pi'$ and where C_i is the constant in the inverse inequality $\|\nabla_h v_h\|_{L^d} \le C_i h^{-1}\|v_h - \pi_h^0 v_h\|_L$ valid for all $v_h \in V_h$, there holds

$$\|u^N - u_h^N\|_L + \left(\sum_{n=0}^{N-1} \tfrac{1}{8}\tau|u_h^n|_S^2 + \tfrac{1}{8}\tau|w_h^n|_S^2\right)^{1/2} \lesssim \tau^2 + h^{3/2}. \tag{3.24}$$

Proof. We bound $\|\xi_h^{n+1} - \zeta_h^n\|_L^2$ differently from the proof of Theorem 3.1. Set $x_h^n := \xi_h^n - \zeta_h^n$, so that (3.16) yields

$$\xi_h^{n+1} - \zeta_h^n = \tfrac{1}{2}\tau L_h x_h^n + \tfrac{1}{2}\tau(\beta_h^n - \alpha_h^n).$$

Hence, using a triangle inequality and Assumption **(A5)** yields

$$\begin{aligned}\|\xi_h^{n+1} - \zeta_h^n\|_L \le{}& \tfrac{1}{2}C_L\sigma\tau\|\nabla_h x_h^n\|_{L^d} + \tfrac{1}{2}C_L\sigma^{1/2}h^{-1/2}\tau|x_h^n|_S \\ &+ \tfrac{1}{2}\tau\|\beta_h^n - \alpha_h^n\|_L.\end{aligned} \tag{3.25}$$

The first step is to control $\|\nabla_h x_h^n\|_{L^d}$. Let $y_h^n = x_h^n - \pi_h^0 x_h^n$ and observe that

$$\|y_h^n\|_L^2 = (x_h^n, y_h^n)_L = \tau(L_h\xi_h^n, y_h^n)_L - \tau(\alpha_h^n, y_h^n)_L,$$

since $x_h^n = \tau L_h \xi_h^n - \tau\alpha_h^n$. To bound the first term in the right-hand side, we use Assumption **(A7)** to infer

$$\tau|(L_h\xi_h^n, y_h^n)_L| \le C_\pi'\sigma^{1/2}h^{-1/2}\tau(|\xi_h^n|_S + \|\xi_h^n\|_L)\|y_h^n\|_L.$$

Furthermore, bounding the second term by a Cauchy–Schwarz inequality, using the CFL condition, and simplifying by $\|y_h^n\|_L$ leads to

$$\|y_h^n\|_L \le C_\pi'\sigma^{1/2}h^{-1/2}\tau|\xi_h^n|_S + \tau\|\alpha_h^n\|_L + C\tau^{1/2}\|\xi_h^n\|_L.$$

Thus,

$$\|\nabla_h x_h^n\|_{L^d} \le C_i h^{-1}\|y_h^n\|_L \le C_i'\sigma^{1/2}h^{-3/2}\tau|\xi_h^n|_S + Ch^{-1}(\tau\|\alpha_h^n\|_L + \tau^{1/2}\|\xi_h^n\|_L),$$

with $C_i' = C_i C_\pi'$. Hence, substituting back into (3.25) yields

$$\|\xi_h^{n+1} - \zeta_h^n\|_L \le \tfrac{1}{2} C_L C_i' \sigma^{3/2} h^{-3/2} \tau^2 |\xi_h^n|_S + \tfrac{1}{2} C_L \sigma^{1/2} h^{-1/2} \tau |\xi_h^n - \zeta_h^n|_S + C\tau^{1/2}(\tau^{5/2} + \|\xi_\pi^n\|_* + \|\zeta_\pi^n\|_* + \|\xi_h^n\|_L),$$

where the contributions of α_h^n and β_h^n have been bounded using (3.19) and the (generic) CFL condition (2.33). Owing to the condition (3.23), it is now inferred that

$$\begin{aligned}\|\xi_h^{n+1} - \zeta_h^n\|_L &\le 2^{-5/2}\tau^{1/2}(|\xi_h^n|_S + |\zeta_h^n - \xi_h^n|_S) + C\tau^{1/2}(\tau^{5/2} + \|\xi_\pi^n\|_* + \|\zeta_\pi^n\|_* + \|\xi_h^n\|_L) \\ &\le 2^{-3/2}\tau^{1/2}(|\xi_h^n|_S + |\zeta_h^n|_S) + C\tau^{1/2}(\tau^{5/2} + \|\xi_\pi^n\|_* + \|\zeta_\pi^n\|_* + \|\xi_h^n\|_L).\end{aligned}$$

Squaring yields

$$\|\xi_h^{n+1} - \zeta_h^n\|_L^2 \le \tfrac{3}{8}\tau |\xi_h^n|_S^2 + \tfrac{3}{8}\tau |\zeta_h^n|_S^2 + C\tau(\tau^5 + \|\xi_\pi^n\|_*^2 + \|\zeta_\pi^n\|_*^2 + \|\xi_h^n\|_L^2).$$

The conclusion readily follows by proceeding as in the proof of Theorem 3.1. □

4. Analysis of explicit RK3 schemes. This section is devoted to the convergence analysis of explicit three-stage RK3 schemes. We proceed similarly to Section 3. The main difference is that a sharper stability estimate can be derived for RK3 schemes, so that the strengthened 4/3-CFL condition (2.34) is no longer needed. Finally, recall that we assume here $u \in C^4(0,T;L)$ and $f \in C^3(0,T;L)$.

4.1. Three-stage RK3 schemes. We consider schemes of the form

$$w_h^n = u_h^n - \tau L_h u_h^n + \tau f_h^n, \tag{4.1}$$

$$y_h^n = \tfrac{1}{2}(u_h^n + w_h^n) - \tfrac{1}{2}\tau L_h w_h^n + \tfrac{1}{2}\tau(f_h^n + \tau\partial_t f_h^n), \tag{4.2}$$

$$u_h^{n+1} = \tfrac{1}{3}(u_h^n + w_h^n + y_h^n) - \tfrac{1}{3}\tau L_h y_h^n + \tfrac{1}{3}\tau\psi_h^n, \tag{4.3}$$

with the assumption that

$$\psi_h^n = f_h^n + \tau\partial_t f_h^n + \tfrac{1}{2}\tau^2\partial_{tt} f_h^n + \delta_h^n, \qquad \|\delta_h^n\|_L \lesssim \tau^3. \tag{4.4}$$

There are many ways of writing explicit three-stage RK3 schemes. Since the space differential operator is linear, they all amount in the homogeneous case ($f = 0$) to

$$u_h^{n+1} = u_h^n - \tau L_h u_h^n + \tfrac{1}{2}\tau^2 L_h^2 u_h^n - \tfrac{1}{6}\tau^3 L_h^3 u_h^n. \tag{4.5}$$

One example that fits the above form is the third-order Heun method which is usually written as follows:

$$k_1 = -L_h u_h^n + f_h^n, \tag{4.6}$$

$$k_2 = -L_h(u_h^n + \tfrac{1}{3}\tau k_1) + f_h^{n+1/3}, \tag{4.7}$$

$$k_3 = -L_h(u_h^n + \tfrac{2}{3}\tau k_2) + f_h^{n+2/3}, \tag{4.8}$$

$$u_h^{n+1} = u_h^n + \tfrac{1}{4}\tau(k_1 + 3k_3). \tag{4.9}$$

Straightforward algebra yields

$$\psi_h^n = -\tfrac{5}{4} f_h^n + \tfrac{9}{4} f_h^{n+2/3} - \tfrac{1}{2}\tau\partial_t f_h^n - \tfrac{3}{2}\tau L_h(f_h^{n+1/3} - f_h^n - \tfrac{1}{3}\tau\partial_t f_h^n). \tag{4.10}$$

PROPOSITION 4.1. *Assume that $f \in C^2(0,T;[H^1(\Omega)]^m)$ and that $s_h = s_h^{\rm cip}$ as defined by* (2.36) *or that $s_h = s_h^{\rm dg}$ as defined by* (2.38)*. Then,* (4.4) *holds.*

Proof. We need to prove that $\|\psi_h^n - (f_h^n + \tau\partial_t f_h^n + \frac{1}{2}\tau^2\partial_{tt} f_h^n)\|_L \lesssim \tau^3$. Set $\psi_h^n = A + B$ with $A = -\frac{5}{4}f_h^n + \frac{9}{4}f_h^{n+2/3} - \frac{1}{2}\tau\partial_t f_h^n$ and $B = -\frac{3}{2}\tau L_h(f_h^{n+1/3} - f_h^n - \frac{1}{3}\tau\partial_t f_h^n)$. Using Taylor expansions yields

$$\|A - (f_h^n + \tau\partial_t f_h^n + \tfrac{1}{2}\tau^2\partial_{tt} f_h^n)\|_L \lesssim \tau^3\|f\|_{C^3(0,T;L)}.$$

Consider now the term B and set $z^n := f^{n+1/3} - f^n - \frac{1}{3}\tau\partial_t f^n$ so that $B = -\frac{3}{2}\tau L_h(\pi_h z^n)$. Assumption **(A5)** yields

$$\|L_h(\pi_h z^n)\|_L \lesssim \|\nabla z^n\|_{L^d} + h^{-1/2}|\pi_h z^n|_S,$$

where we have used the H^1-stability of π_h in writing $\|\nabla z^n\|_{L^d}$. When $s_h = s_h^{\mathrm{dg}}$, observe that $|z^n|_S = 0$ since $f \in C^2(0,T;[H^1(\Omega)]^m)$ so that

$$h^{-1/2}|\pi_h z^n|_S = h^{-1/2}|z^n - \pi_h z^n|_S \lesssim \|\nabla z^n\|_{L^d}.$$

When $s_h = s_h^{\mathrm{cip}}$, the boundary contribution is bounded as above, while the interior contribution is bounded by a trace inequality and the H^1-stability of π_h, yielding again $h^{-1/2}|\pi_h z^n|_S \lesssim \|\nabla z^n\|_{L^d}$. As a result, using Taylor expansions yields

$$\|B\|_L \lesssim \tau\|\nabla(f^{n+1/3} - f^n - \tfrac{1}{3}\tau\partial_t f^n)\|_{L^d} \lesssim \tau^3\|f\|_{C^2(0,T;[H^1(\Omega)]^m)},$$

completing the proof. ∎

4.2. The error equation. Along with definitions (3.10) and (3.11), let

$$\theta_h^n = y_h^n - \pi_h y^n, \qquad \theta_\pi^n = y^n - \pi_h y^n, \tag{4.11}$$

with $y = u + \tau\partial_t u + \frac{1}{2}\tau^2\partial_{tt} u$.

LEMMA 4.1. *There holds*

$$\zeta_h^n = \xi_h^n - \tau L_h \xi_h^n + \tau\alpha_h^n, \tag{4.12}$$

$$\theta_h^n = \tfrac{1}{2}(\xi_h^n + \zeta_h^n) - \tfrac{1}{2}\tau L_h\zeta_h^n + \tfrac{1}{2}\tau\beta_h^n, \tag{4.13}$$

$$\xi_h^{n+1} = \tfrac{1}{3}(\xi_h^n + \zeta_h^n + \theta_h^n) - \tfrac{1}{3}\tau L_h\theta_h^n + \tfrac{1}{3}\tau\gamma_h^n, \tag{4.14}$$

with

$$\alpha_h^n = L_h\xi_\pi^n, \qquad \beta_h^n = L_h\zeta_\pi^n, \qquad \gamma_h^n = L_h\theta_\pi^n - \pi_h\eta^n + \delta_h^n, \tag{4.15}$$

where $\eta^n = \tau^{-1}\int_{I_n}\frac{1}{2}(t_{n+1} - t)^3\partial_{tttt}u\,dt$.

Proof. Equations (4.12) and (4.13) are obtained as in Lemma 3.1. To derive (4.14), observe that

$$u^{n+1} = u^n + \tau\partial_t u^n + \tfrac{1}{2}\tau^2\partial_{tt}u^n + \tfrac{1}{6}\tau^3\partial_{ttt}u^n + \tfrac{1}{3}\tau\eta^n,$$

and proceed again as in Lemma 3.1. ∎

For further use, it is convenient to recall that (4.12)–(4.13) imply

$$\theta_h^n = \zeta_h^n - \tfrac{1}{2}\tau L_h(\zeta_h^n - \xi_h^n) + \tfrac{1}{2}\tau(\beta_h^n - \alpha_h^n), \tag{4.16}$$

and to observe that (4.13)–(4.14) imply

$$\xi_h^{n+1} = \theta_h^n - \tfrac{1}{3}\tau L_h(\theta_h^n - \zeta_h^n) + \tfrac{1}{3}\tau(\gamma_h^n - \beta_h^n). \tag{4.17}$$

4.3. Energy identity and stability. Our goal is now to derive an energy identity, then leading to our main stability estimate.

LEMMA 4.2 (Energy identity). *There holds*

$$\begin{aligned}\tfrac{1}{2}\|\xi_h^{n+1}\|_L^2 - \tfrac{1}{2}\|\xi_h^n\|_L^2 + \tfrac{1}{2}\tau|\xi_h^n|_S^2 + \tfrac{1}{6}\tau|\zeta_h^n|_S^2 + \tfrac{1}{3}\tau|\theta_h^n|_S^2 + \tfrac{1}{6}\|\theta_h^n - \zeta_h^n\|_L^2 \\ = \tfrac{1}{6}\tau|\zeta_h^n - \xi_h^n|_S^2 + \tfrac{1}{2}\|\xi_h^{n+1} - \theta_h^n\|_L^2 + \Lambda_h^n \\ + \tfrac{1}{3}\tau(\gamma_h^n, \theta_h^n)_L + \tfrac{1}{6}\tau(\beta_h^n, \xi_h^n)_L + \tfrac{1}{3}\tau(\alpha_h^n, \xi_h^n + \tfrac{1}{2}\zeta_h^n)_L,\end{aligned} \tag{4.18}$$

where $\Lambda_h^n := \frac{1}{6}\tau(\Lambda\xi_h^n, \xi_h^n)_L - \frac{1}{6}\tau(\Lambda\zeta_h^n, \xi_h^n)_L + \frac{1}{6}\tau(\Lambda\theta_h^n, \theta_h^n)_L$.

REMARK 4.1. *The quantities* $\frac{1}{6}\tau|\zeta_h^n - \xi_h^n|_S^2$ *and* $\frac{1}{2}\|\xi_h^{n+1} - \theta_h^n\|_L^2$ *appearing in the right-hand side of the energy identity* (4.18) *are the anti-dissipative terms associated with the explicit nature of the RK3 scheme. However, contrary to the RK2 scheme, there is now a positive term in the left-hand side of* (4.18)*, namely* $\frac{1}{6}\|\theta_h^n - \zeta_h^n\|_L^2$*, which significantly improves the stability properties of the RK3 scheme, in particular circumventing the need for the strengthened 4/3-CFL condition for high-order polynomials.*

Proof. Set $A = \frac{1}{2}\|\xi_h^{n+1}\|_L^2 - \frac{1}{2}\|\xi_h^{n+1} - \theta_h^n\|_L^2 - \frac{1}{2}\|\xi_h^n\|_L^2$. Then,

$$\begin{aligned}A &= (\xi_h^{n+1} - \tfrac{1}{2}\theta_h^n, \theta_h^n)_L - \tfrac{1}{2}\|\xi_h^n\|_L^2 \\ &= \tfrac{1}{2}\|\theta_h^n\|_L^2 + (\xi_h^{n+1} - \theta_h^n, \theta_h^n)_L - \tfrac{1}{2}\|\xi_h^n\|_L^2 \\ &= \tfrac{1}{2}\|\theta_h^n\|_L^2 - \tfrac{1}{2}\|\xi_h^n\|_L^2 - \tfrac{1}{3}\tau(L_h(\theta_h^n - \zeta_h^n), \theta_h^n)_L + \tfrac{1}{3}\tau(\gamma_h^n - \beta_h^n, \theta_h^n)_L,\end{aligned}$$

where (4.17) has been used. Set

$$D_1 := \tfrac{1}{3}\tau(\gamma_h^n - \beta_h^n, \theta_h^n)_L.$$

The term $\frac{1}{2}\|\theta_h^n\|_L^2 - \frac{1}{2}\|\xi_h^n\|_L^2$ can be evaluated using the energy identity (3.17) for the RK2 scheme upon replacing ξ_h^{n+1} by θ_h^n. Setting

$$D_2 := D_1 + \tfrac{1}{2}\tau(\alpha_h^n, \xi_h^n)_L + \tfrac{1}{2}\tau(\beta_h^n, \zeta_h^n)_L + \tfrac{1}{4}\tau(\Lambda\xi_h^n, \xi_h^n)_L + \tfrac{1}{4}\tau(\Lambda\zeta_h^n, \zeta_h^n)_L,$$

yields

$$\begin{aligned}A &= -\tfrac{1}{2}\tau|\xi_h^n|_S^2 - \tfrac{1}{2}\tau|\zeta_h^n|_S^2 + \tfrac{1}{2}\|\theta_h^n - \zeta_h^n\|_L^2 - \tfrac{1}{3}\tau(L_h(\theta_h^n - \zeta_h^n), \theta_h^n)_L + D_2 \\ &= -\tfrac{1}{2}\tau|\xi_h^n|_S^2 - \tfrac{1}{2}\tau|\zeta_h^n|_S^2 - \tfrac{1}{3}\tau|\theta_h^n|_S^2 + \tfrac{1}{2}\|\theta_h^n - \zeta_h^n\|_L^2 + \tfrac{1}{3}\tau(L_h\zeta_h^n, \theta_h^n)_L + D_2' \\ &= -\tfrac{1}{2}\tau|\xi_h^n|_S^2 - \tfrac{1}{6}\tau|\zeta_h^n|_S^2 - \tfrac{1}{3}\tau|\theta_h^n|_S^2 + \tfrac{1}{2}\|\theta_h^n - \zeta_h^n\|_L^2 + \tfrac{1}{3}\tau(L_h\zeta_h^n, \theta_h^n - \zeta_h^n)_L + D_2'' \\ &= -\tfrac{1}{2}\tau|\xi_h^n|_S^2 - \tfrac{1}{6}\tau|\zeta_h^n|_S^2 - \tfrac{1}{3}\tau|\theta_h^n|_S^2 + \tfrac{1}{2}(\theta_h^n - \zeta_h^n, \theta_h^n - \zeta_h^n + \tfrac{2}{3}\tau L_h\zeta_h^n)_L + D_2'',\end{aligned}$$

with $D_2' := D_2 + \frac{1}{6}\tau(\Lambda\theta_h^n, \theta_h^n)_L$ and $D_2'' := D_2' - \frac{1}{6}\tau(\Lambda\zeta_h^n, \zeta_h^n)_L$. Consider the fourth term in the right-hand side, say B, and observe that owing to (4.12) and (4.16),

$$\begin{aligned}B &= \tfrac{1}{2}(\theta_h^n - \zeta_h^n, -\tfrac{1}{3}(\theta_h^n - \zeta_h^n) + \tfrac{2}{3}\tau L_h\xi_h^n + \tfrac{2}{3}\tau(\beta_h^n - \alpha_h^n))_L \\ &= -\tfrac{1}{6}\|\theta_h^n - \zeta_h^n\|_L^2 + \tfrac{1}{3}(\theta_h^n - \zeta_h^n, \xi_h^n - \zeta_h^n)_L + \tfrac{1}{3}\tau(\beta_h^n, \theta_h^n - \zeta_h^n)_L.\end{aligned}$$

Set $G = -\frac{1}{2}\tau|\xi_h^n|_S^2 - \frac{1}{6}\tau|\zeta_h^n|_S^2 - \frac{1}{3}\tau|\theta_h^n|_S^2 - \frac{1}{6}\|\theta_h^n - \zeta_h^n\|_L^2$ and $D_3 = D_2'' + \frac{1}{3}\tau(\beta_h^n, \theta_h^n - \zeta_h^n)_L$, so that

$$A = G + \tfrac{1}{3}(\theta_h^n - \zeta_h^n, \xi_h^n - \zeta_h^n)_L + D_3.$$

Then, using again (4.16) leads to

$$\begin{aligned} A &= G + \tfrac{1}{3}(-\tfrac{1}{2}\tau L_h(\zeta_h^n - \xi_h^n) + \tfrac{1}{2}\tau(\beta_h^n - \alpha_h^n), \xi_h^n - \zeta_h^n)_L + D_3 \\ &= G + \tfrac{1}{6}\tau|\zeta_h^n - \xi_h^n|_S^2 + D_4, \end{aligned}$$

with $D_4 = D_3 + \frac{1}{6}\tau(\beta_h^n - \alpha_h^n, \xi_h^n - \zeta_h^n)_L - \frac{1}{12}\tau(\Lambda(\zeta_h^n - \xi_h^n), \zeta_h^n - \xi_h^n)_L$. Using the expressions for D_1, D_2'', and D_3 in D_4 yields (4.18). □

LEMMA 4.3 (Stability). *Under the usual CFL condition* (2.33) *with*

$$\varrho \le \min(\tfrac{5}{154}C_S^{-1}, (\tfrac{3}{4})^{1/2}C_{L*}^{-1}), \tag{4.19}$$

there holds

$$\begin{aligned} \|\xi_h^{n+1}\|_L^2 - \|\xi_h^n\|_L^2 + \tfrac{1}{48}\tau|\xi_h^n|_S^2 + \tfrac{1}{12}\tau|\zeta_h^n|_S^2 + \tfrac{1}{48}\tau|\theta_h^n|_S^2 \\ \le C\tau(\tau^6 + \|\xi_\pi^n\|_*^2 + \|\zeta_\pi^n\|_*^2 + \|\theta_\pi^n\|_*^2 + \|\xi_h^n\|_L^2). \end{aligned} \tag{4.20}$$

Proof. We bound the terms in the right-hand side of the energy identity (4.18).
(i) Bound on $\frac{1}{6}\tau|\zeta_h^n - \xi_h^n|_S^2$. Let ϵ and $\hat\epsilon$ be positive real numbers to be chosen later. Observe that

$$\begin{aligned} |\zeta_h^n - \xi_h^n|_S^2 &\le (1+\epsilon)|\theta_h^n - \xi_h^n|_S^2 + (1+\epsilon^{-1})|\theta_h^n - \zeta_h^n|_S^2 \\ &\le (1+\epsilon)(1+\hat\epsilon)|\theta_h^n|_S^2 + (1+\epsilon)(1+\hat\epsilon^{-1})|\xi_h^n|_S^2 + (1+\epsilon^{-1})|\theta_h^n - \zeta_h^n|_S^2 \\ &\le (1+\epsilon)(1+\hat\epsilon)|\theta_h^n|_S^2 + (1+\epsilon)(1+\hat\epsilon^{-1})|\xi_h^n|_S^2 \\ &\quad + (1+\epsilon^{-1})C_S\sigma h^{-1}\|\theta_h^n - \zeta_h^n\|_L^2, \end{aligned}$$

where Assumption **(A4)** has been used. Then, taking $\epsilon = \frac{5}{72}$ and $\hat\epsilon = \frac{7}{11}$ and observing that $\frac{1}{6}(1+\epsilon)(1+\hat\epsilon) = \frac{7}{24}$, $\frac{1}{6}(1+\epsilon)(1+\hat\epsilon^{-1}) = \frac{11}{24}$, and that

$$\tfrac{1}{6}\tau(1+\epsilon^{-1})C_S\sigma h^{-1} \le \tfrac{1}{12},$$

owing to the choice (4.19) for the CFL condition, it is inferred that

$$\tfrac{1}{6}\tau|\zeta_h^n - \xi_h^n|_S^2 \le \tfrac{7}{24}\tau|\theta_h^n|_S^2 + \tfrac{11}{24}\tau|\xi_h^n|_S^2 + \tfrac{1}{12}\|\theta_h^n - \zeta_h^n\|_L^2.$$

(ii) Bound on $\frac{1}{2}\|\xi_h^{n+1} - \theta_h^n\|_L^2$. Using (4.17) and the bound (2.31) yields

$$\begin{aligned} \tfrac{1}{2}\|\xi_h^{n+1} - \theta_h^n\|_L^2 &\le \tfrac{1}{9}\tau^2\|L_h(\theta_h^n - \zeta_h^n)\|_L^2 + \tfrac{1}{9}\tau^2\|\gamma_h^n - \beta_h^n\|_L^2 \\ &\le \tfrac{1}{9}(\tau C_{L*}\sigma h^{-1})^2\|\theta_h^n - \zeta_h^n\|_L^2 + \tfrac{1}{9}\tau^2\|\gamma_h^n - \beta_h^n\|_L^2 \\ &\le \tfrac{1}{12}\|\theta_h^n - \zeta_h^n\|_L^2 + \tfrac{1}{9}\tau^2\|\gamma_h^n - \beta_h^n\|_L^2, \end{aligned}$$

owing to the choice (4.19) for the CFL condition.
(iii) Inserting the bounds delivered in steps (i) and (ii) into (4.18) yields

$$\begin{aligned} &\tfrac{1}{2}\|\xi_h^{n+1}\|_L^2 - \tfrac{1}{2}\|\xi_h^n\|_L^2 + \tfrac{1}{24}\tau|\xi_h^n|_S^2 + \tfrac{1}{6}\tau|\zeta_h^n|_S^2 + \tfrac{1}{24}\tau|\theta_h^n|_S^2 \\ &\quad \le \tfrac{1}{9}\tau^2\|\gamma_h^n - \beta_h^n\|_L^2 + \tfrac{1}{3}\tau(\gamma_h^n, \theta_h^n)_L + \tfrac{1}{6}\tau(\beta_h^n, \xi_h^n)_L + \tfrac{1}{3}\tau(\alpha_h^n, \xi_h^n + \tfrac{1}{2}\zeta_h^n)_L + \Lambda_h^n. \end{aligned}$$

(iv) It remains to bound the five terms in the right-hand side, say T_1–T_5. To this purpose, we first bound the quantities α_h^n, β_h^n, and γ_h^n by proceeding as for the RK2 scheme. It is readily inferred that

$$\tau\|\alpha_h^n\|_L \lesssim \tau^{1/2}\|\xi_\pi^n\|_*, \quad \tau\|\beta_h^n\|_L \lesssim \tau^{1/2}\|\zeta_\pi^n\|_*, \quad \tau\|\gamma_h^n\|_L \lesssim \tau^{1/2}\|\theta_\pi^n\|_* + \tau^4,$$

and that for all $v_h \in V_h$,

$$\begin{aligned}
\tau(\alpha_h^n, v_h)_L &\lesssim \tau\|\xi_\pi^n\|_*(|v_h|_S + \|v_h\|_L),\\
\tau(\beta_h^n, v_h)_L &\lesssim \tau\|\zeta_\pi^n\|_*(|v_h|_S + \|v_h\|_L),\\
\tau(\gamma_h^n, v_h)_L &\lesssim \tau\|\theta_h^n\|_*(|v_h|_S + \|v_h\|_L) + \tau^4\|v_h\|_L.
\end{aligned}$$

Moreover, still proceeding as for the RK2 scheme,

$$\|\zeta_h^n\|_L \lesssim \|\xi_h^n\|_L + \|\xi_\pi\|_*, \qquad \|\theta_h^n\|_L \lesssim \|\xi_h^n\|_L + \|\xi_\pi\|_* + \|\zeta_\pi^n\|_*.$$

Using these estimates yields

$$T_1 \lesssim \tau(\tau^7 + \|\zeta_\pi^n\|_*^2 + \|\theta_\pi^n\|_*^2).$$

Furthermore, using Young inequalities leads to

$$\begin{aligned}
T_2 + T_3 + T_4 \le \tfrac{1}{48}\tau|\xi_h^n|_S^2 + \tfrac{1}{12}\tau|\zeta_h^n|_S^2 + \tfrac{1}{48}\tau|\theta_h^n|_S^2 \\
+ C\tau(\tau^6 + \|\xi_\pi^n\|_*^2 + \|\zeta_\pi^n\|_*^2 + \|\theta_\pi^n\|_*^2 + \|\xi_h^n\|_L^2).
\end{aligned}$$

Finally, since Λ is symmetric,

$$T_5 \lesssim \tau(\|\xi_h^n\|_L^2 + \|\zeta_h^n\|_L^2 + \|\theta_h^n\|_L^2) \lesssim \tau(\|\xi_\pi^n\|_*^2 + \|\zeta_\pi^n\|_*^2 + \|\xi_h^n\|_L^2).$$

Collecting the above bounds and since $\tau^7 \le \tau^6$ concludes the proof. ∎

4.4. Error estimate. The next theorem provides a general *a priori* error estimate under the usual CFL condition.

THEOREM 4.1. *Assume that* $u \in C^4(0,T;L) \cap C^0(0,T;[H^{p+1}(\Omega)]^m)$. *Under the CFL condition* (2.33) *with the choice* (4.19) *for* ϱ, *there holds*

$$\|u^N - u_h^N\|_L + \left(\sum_{n=0}^{N-1} \tfrac{1}{48}\tau|u_h^n|_S^2 + \tfrac{1}{12}\tau|w_h^n|_S^2 + \tfrac{1}{48}\tau|y_h^n|_S^2\right)^{1/2} \lesssim \tau^3 + h^{p+1/2}. \quad (4.21)$$

Proof. Starting with estimate (4.20), sum over n, apply Gronwall's lemma, and use the approximation property (2.32). ∎

5. Numerical results. In this section we investigate numerically the explicit RK2 and RK3 schemes using, respectively, their implementations (3.6)-(3.8) and (4.6)-(4.9). Regarding space discretization, we consider the continuous (CIP stabilized) and discontinuous (DG) finite element methods discussed in §2.4, using piecewise affine ($p = 1$) and quadratic ($p = 2$) polynomials. We first illustrate the convergence properties of the various schemes by considering two test cases with analytical smooth solutions. Then, we investigate on a benchmark with rough solution the capability of the present schemes to control spurious oscillations. The numerical computations have been carried out using FreeFem++ [21].

5.1. Convergence rates for smooth solutions. We focus on two of the examples discussed in §2.1, namely the advection and acoustics equations.

To illustrate the convergence rate of the discrete solutions, we have computed the energy errors $\|u^N - u_h^N\|_L$ at the final simulation time for specific sequences of τ- and $h-$refinements. The scaling τ/h is chosen to satisfy the appropriate CFL condition and, according to the error estimates (3.22), (3.24) or (4.21), in such a way that the error in time dominates the error in space. More precisely, we have taken:

- For RK2 with $p = 1$ and RK3 with $p = 2$, $\tau = Ch$ (constant usual CFL);
- For RK2 with $p = 2$, $\tau = Ch^{4/3}$ (constant strengthened 4/3-CFL);
- For RK3 with $p = 1$, $\tau = Ch^{1/2}$. This choice is made in order to reduce the spatial error which scales as $h^{3/2}$ only. The usual CFL increases as the time step is reduced; for the smallest time step considered, we have ensured that the scaling τ/h satisfies the required condition (4.19).

5.1.1. Advection equation. As a first numerical test, we consider a two-dimensional rotating Gaussian benchmark: we solve (2.10) with $\beta = (y, x)^{\mathrm{t}}$, $f = 0$, $\Omega = \{(x, y) \in \mathbb{R}^2 : x^2 + y^2 \leq 1\}$, and the following Gaussian function, centered at the point $(0.3, 0.3)$,

$$u_0(x, y) = e^{10[(x-0.3)^2+(y-0.3)^2]},$$

as initial condition. The stabilization parameter γ in S_F^{int} is set to 0.5 for DG (i.e., upwinding), and to 0.005 and 0.001 for CIP with $p = 1$ and $p = 2$, respectively (improvements by further tuning of these parameters goes beyond the present scope; see, e.g., [4] for such an investigation in the steady case). For each numerical scheme, we report the energy errors at the final time $T = 2\pi$, i.e., after a complete rotation of the initial condition.

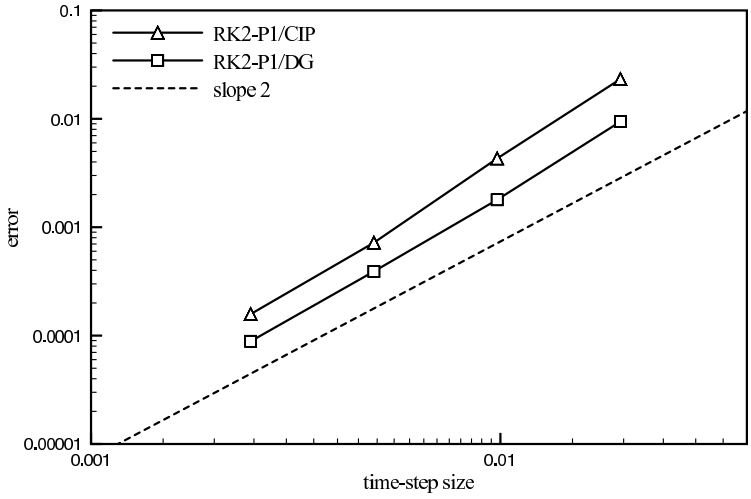

FIGURE 5.1. *Advection equation. Convergence history for explicit RK2 with continuous (CIP) and discontinuous (DG) affine finite elements ($p = 1$).*

	(h, τ)	$(h, \tau)/2$	$(h, \tau)/4$	$(h, \tau)/8$
CIP	0.4	7	54	568
DG	1.6	11	90	781

TABLE 5.1

Advection equation. Elapsed CPU time (dimensionless) for the computation of the results reported in Figure 5.1.

Figure 5.1 presents the convergence results for the RK2 scheme with $p = 1$. We have set $\tau/h = 0.2$, which amounts to choosing $\varrho = 0.2$ in the usual CFL condition (2.33) (recall that, here, $\sigma = 1$). The RK2-CIP and the RK2-DG schemes exhibit second-order accuracy in time, as stated in Theorem 3.2. On a fixed mesh, the DG formulation yields more accurate results, together with increased computational cost. This is reflected in Table 5.1 which reports the corresponding (dimensionless) CPU times. The increased accuracy and cost of the DG formulation can be related to the larger number of degrees of freedom. In this sense, it is worth noticing that all the linear systems have been solved using the sparse direct solver provided with FreeFem++ without explicitly exploiting the block diagonal structure of the DG mass matrix (this is particularly relevant in large-scale computations).

The convergence results for the RK2 scheme with quadratic finite elements ($p = 2$) are presented in Figure 5.2. Here, the discretization parameters τ and h satisfy the strengthened 4/3-CFL condition (2.34) with $\varrho' = 0.14$. As expected, the RK2-CIP and RK2-DG schemes exhibit the $O(\tau^2)$ accuracy predicted by Theorem 3.1. We also observe that the strengthened 4/3-CFL condition seems to be numerically sharp.

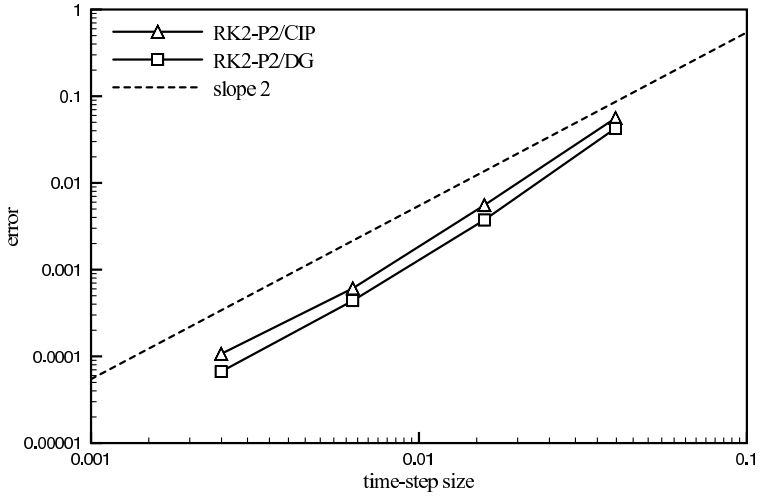

FIGURE 5.2. *Advection equation. Convergence history for explicit RK2 with continuous (CIP) and discontinuous (DG) quadratic finite elements* ($p = 2$).

Figure 5.3 presents the results for the RK3 scheme with affine finite elements ($p = 1$). Here, τ scales as $h^{1/2}$ and the usual CFL condition is satisfied with an increasing parameter ϱ, up to 0.21. Surprisingly, both the RK3-CIP and the RK3-DG schemes show a convergence rate higher than the theoretical $O(\tau^3)$ stated in Theorem 4.1. A possible explanation is that contributions of the spatial error can be dominant on the coarser meshes. Finally, Figure 5.4 reports the results for RK3 with quadratic finite elements ($p = 2$). Here, the usual CFL condition (2.33) holds with $\varrho = 0.08$. Both the RK3-CIP and the RK3-DG schemes exhibit the $O(\tau^3)$ accuracy stated in Theorem 4.1, although some perturbations, due to the $O(h^{5/2})$ spatial contribution of error, are clearly visible on the finer meshes.

5.1.2. Wave equation. We now consider the first-order PDE system (2.15) in the unit square $\Omega = [0, 1]^2$ with reference velocity $c_0 = 1$ and final simulation time

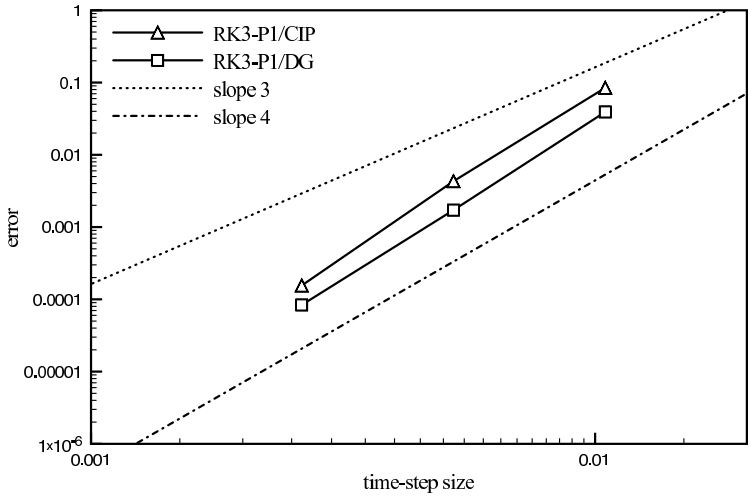

FIGURE 5.3. *Advection equation. Convergence history for explicit RK3 with continuous (CIP) and discontinuous (DG) affine finite elements* ($p = 1$).

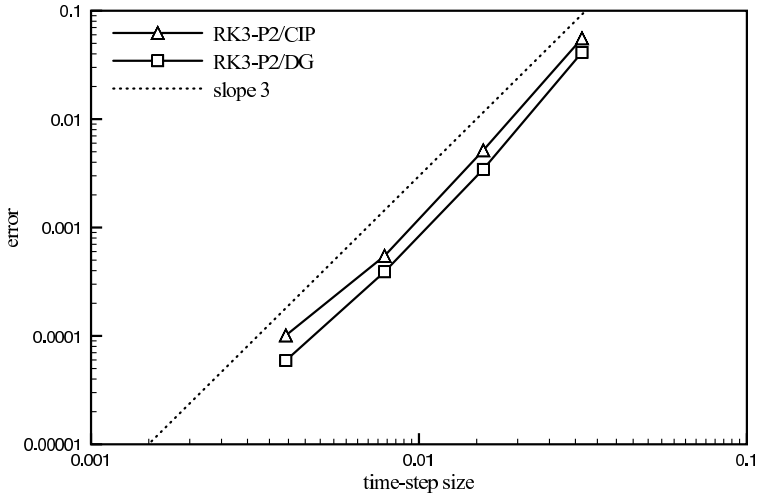

FIGURE 5.4. *Advection equation. Convergence history for explicit RK3 with continuous (CIP) and discontinuous (DG) quadratic finite elements* ($p = 2$).

$T = 1$. The right-hand sides f_1 and f_2 and the initial data are chosen to yield the following exact solution:

$$p(x, y, t) = \exp(t)\sin(\pi x)\sin(\pi y), \qquad q(x, y, t) = p(x, y, t)\begin{bmatrix}1\\1\end{bmatrix}.$$

For the DG method, the free parameters in S_F^{ext} and S_F^{int} are set to $\gamma_1 = 1$ and $\gamma_2 = \gamma_3 = 0.1$, while for the CIP method, they are set to $\gamma_1 = 1$ and $\gamma_2 = \gamma_3 = 0.01$ with $p = 1$ and $\gamma_2 = \gamma_3 = 0.005$ with $p = 2$. In Figures 5.5 to 5.8, we report the

convergence results for the energy norm of the error at final time.

The RK2 scheme with affine finite elements ($p = 1$) exhibits optimal time convergence, as shown in Figure 5.5. Here, the discretization parameters satisfy the usual CFL constraint with $\varrho = 0.13$. The same optimal rate is obtained in Figure 5.6 with quadratic finite elements ($p = 2$) and a set of time and space meshes satisfying the strengthened 4/3-CFL condition with $\varrho' = 0.07$.

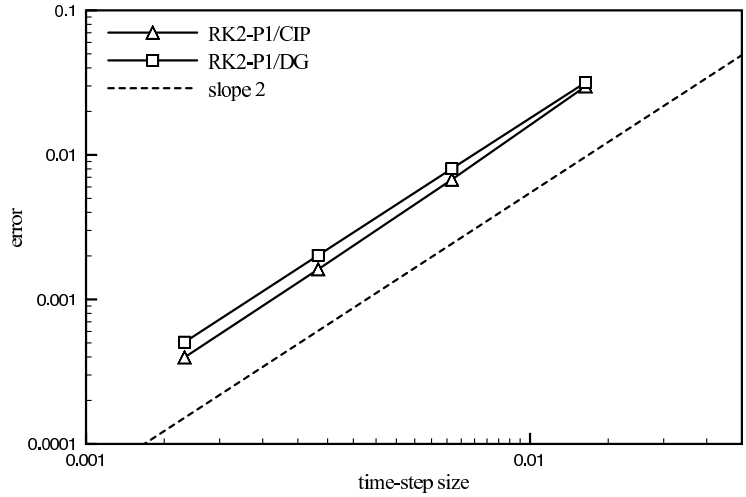

FIGURE 5.5. *Wave equation. Convergence history for explicit RK2 with continuous (CIP) and discontinuous (DG) affine finite elements.*

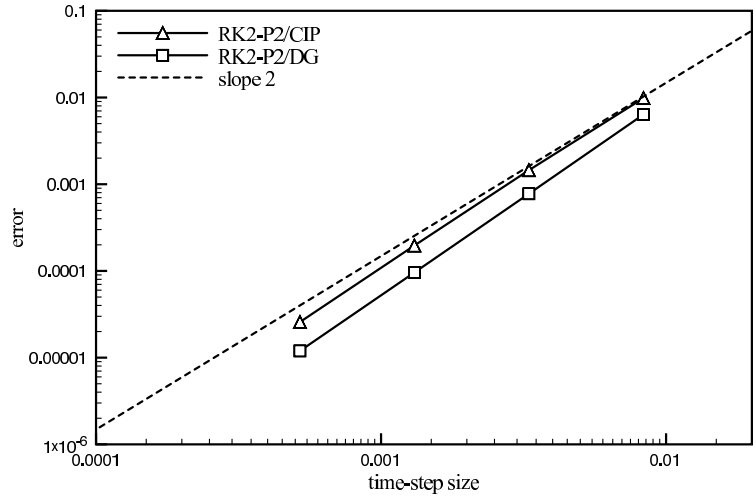

FIGURE 5.6. *Wave equation. Convergence history for explicit RK2 with continuous (CIP) and discontinuous (DG) quadratic finite elements.*

As in the rotating Gaussian benchmark, a super-convergence behavior is obtained

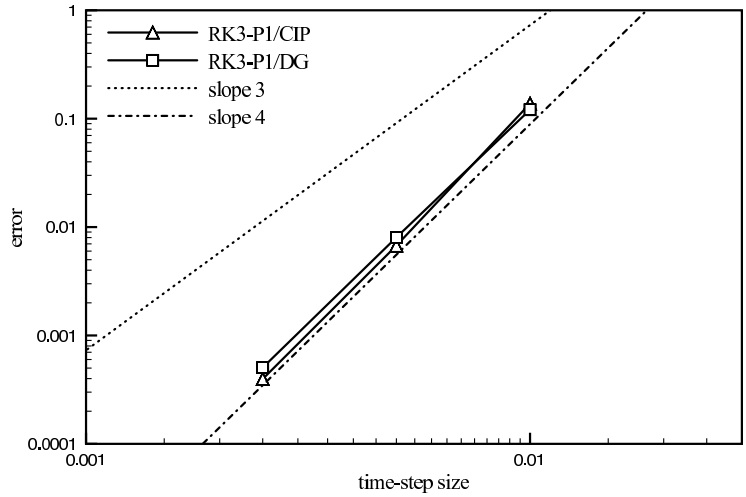

FIGURE 5.7. *Wave equation. Convergence history for explicit RK3 with continuous (CIP) and discontinuous (DG) affine finite elements.*

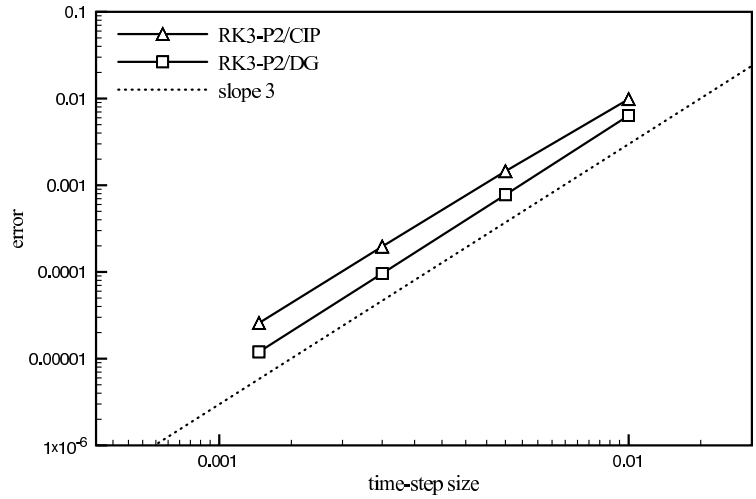

FIGURE 5.8. *Wave equation. Convergence history for explicit RK3 with continuous (CIP) and discontinuous (DG) quadratic finite elements.*

for the RK3 scheme and affine finite elements ($p = 1$), see Figure 5.7. The time step τ scales as $h^{1/2}$ and the usual CFL is satisfied with an increasing parameter ϱ, up to 0.21. Finally, Figure 5.8 presents the results for RK3 with quadratic finite elements ($p = 2$) and the usual CFL condition holding with $\varrho = 0.05$. Optimal $O(\tau^3)$ accuracy is obtained for the CIP and the DG discretizations.

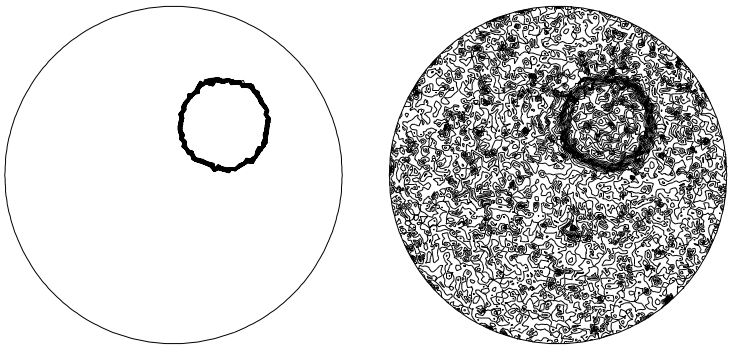

(a) Discrete initial condition (b) RK2-$\mathbb{P}_1$/Unstabilized

FIGURE 5.9. *Contour-lines for the discrete initial condition and the final discrete solution provided by the explicit RK2 scheme with unstabilized continuous affine finite elements.*

5.2. Controlling oscillations in rough solutions. For the advection benchmark discussed in §5.1.1, we now consider the following initial data:

$$u_0(x,y) = \frac{1}{2}\left[\tanh\left(\frac{e^{-10[(x-0.3)^2+(y-0.3)^2]}-0.5}{0.001}\right)+1\right].$$

This function is smooth but has a sharp layer (with thickness of order 0.001) leading to spurious oscillations when using unstabilized continuous finite elements on meshes that are too coarse to resolve the internal layer. Our goal with this test case is to illustrate the capabilities of the methods analyzed in this paper to control such spurious oscillations. To this aim, we consider a fixed uniform mesh with 256 elements along the boundary of Ω ($h \approx 0.025$). The sharp layer is thus under-resolved. The discrete initial data takes the form of a cylinder of height 1 centered at the point $(0.3, 0.3)$; the contour-lines of its linear interpolant are shown in Figure 5.9a. Figure 5.9b shows the solution at final time, $T = 2\pi$ (i.e., after one rotation of the initial data), obtained by the explicit RK2 scheme (1000 time steps) with unstabilized continuous, piecewise affine finite elements ($\gamma = 0$ in the CIP method). The numerical solution is globally polluted by spurious oscillations.

In Figure 5.10 we report the approximate solutions obtained with the explicit RK2 scheme, using piecewise affine or quadratic CIP or DG finite elements and using the largest allowed (in terms of stability) time step size τ. As expected, global oscillations are eliminated by both the CIP and the DG methods, and the numerical solution maintains its general aspect with a sharp layer. The increased accuracy of CIP and DG with $p = 2$ is clearly visible. Note that, compared to DG and for the considered values of γ, the CIP method allows the use of larger time steps. Moreover, the critical value of τ depends on the polynomial order.

In Figure 5.11 we have finally reported the approximate solutions obtained with the explicit RK3 scheme. Note the slightly improved accuracy with respect to Figure 5.10. Once more, the critical value of τ depends on the polynomial order and the largest values were obtained with the CIP method (for the considered choice of the stabilization parameter).

6. Concluding remarks. In this work, we have analyzed several approximation methods to the evolution problem (1.1) combining explicit RK schemes in time and

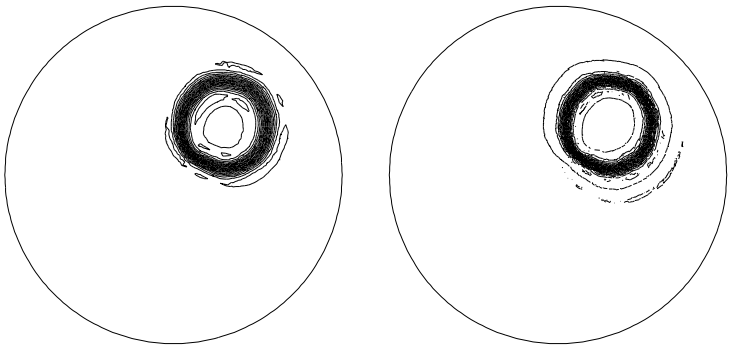

(a) RK2-$\mathbb{P}_1$/CIP, $\tau/h = 0.51$ (b) RK2-$\mathbb{P}_1$/DG, $\tau/h = 0.2$

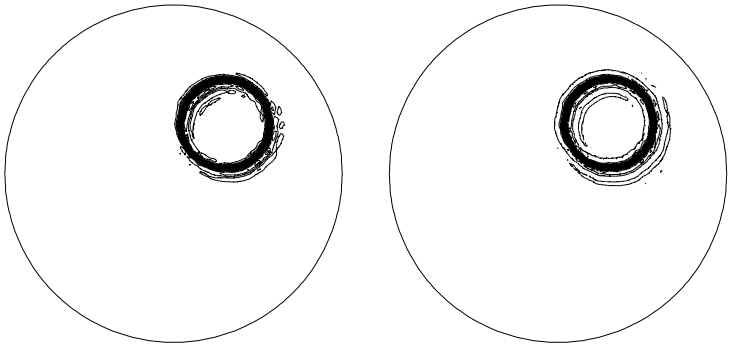

(c) RK2-$\mathbb{P}_2$/CIP, $\tau/h = 0.2$ (d) RK2-$\mathbb{P}_2$/DG, $\tau/h = 0.12$

FIGURE 5.10. *Contour-lines of the final discrete solution obtained with the explicit RK2 scheme and piecewise affine or quadratic CIP stabilized or DG finite elements.*

stabilized finite elements in space. A series of numerical tests confirmed the stated stability and convergence results. In our opinion, salient features of this work are the following: (i) the fact that continuous and discontinuous finite element approximation in space can be cast into a unified analysis framework, (ii) the possibility to use high-order approximation methods in space and time (at least up to third-order in time, but an extension to RK4 schemes proceeding along the same lines should be feasible) in an explicit framework, (iii) the intertwined stability effects coupling stabilization in space and anti-dissipativity in time. This last point is particularly evident in the analysis of RK2 schemes with piecewise affine finite elements, but it also plays a role in bounding the α_h^n, β_h^n, and γ_h^n terms in the energy identities owing to Assumption **(A6)**.

Extensions of this work can explore various directions. Firstly, a more general form for the evolution problem (1.1) can be considered, namely

$$A_0\partial_t u + Au = f \qquad \text{on } \Omega \times (0,T). \tag{6.1}$$

When A_0 is smooth, the above analysis carries over with minor modifications. When A_0 is not smooth (e.g., piecewise constant on the mesh), the analysis must be modified; DG methods appear to be more appropriate to handle this case. A further extension of the present analysis is to tackle error estimates in the graph norm. Finally, ongoing work focuses on combining explicit and implicit schemes for the approximation of evolution problems with stiff terms resulting from diffusion or strong reaction.

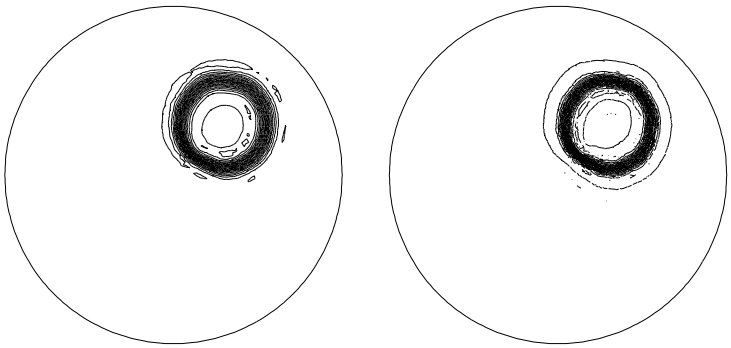

(a) RK3-$\mathbb{P}_1$/CIP, $\tau/h = 0.64$ (b) RK3-$\mathbb{P}_1$/DG, $\tau/h = 0.26$

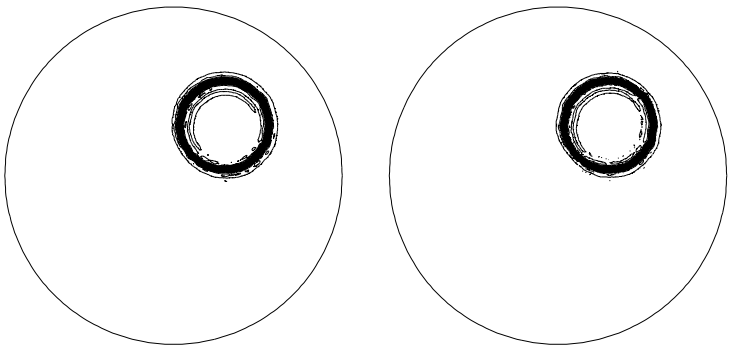

(c) RK3-$\mathbb{P}_2$/CIP, $\tau/h = 0.26$ (d) RK3-$\mathbb{P}_2$/DG, $\tau/h = 0.15$

FIGURE 5.11. *Contour-lines of the final discrete solution obtained with the explicit RK3 scheme and piecewise affine or quadratic CIP stabilized or DG finite elements.*

Acknowledgments. This work was partly supported by the Groupement MoMaS (PACEN/CNRS, ANDRA, BRGM, CEA, EdF, IRSN). The first author acknowledges support from INRIA and Université Paris-Est during his stays as an invited professor in September 2008 and 2009.

REFERENCES

[1] M. Braack, E. Burman, V. John, and G. Lube. Stabilized finite element methods for the generalized Oseen problem. *Comput. Methods Appl. Mech. Engrg.*, 196(4-6):853–866, 2007.

[2] E. Burman. A unified analysis for conforming and nonconforming stabilized finite element methods using interior penalty. *SIAM J. Numer. Anal.*, 43(5):2012–2033 (electronic), 2005.

[3] E. Burman and P. Hansbo. Edge stabilization for Galerkin approximations of convection–diffusion–reaction problems. *Comput. Methods Appl. Mech. Engrg.*, 193:1437–1453, 2004.

[4] E. Burman, A. Quarteroni, and B. Stamm. Interior penalty continuous and discontinuous finite element approximations of hyperbolic equations. *J. Sci. Comput.* DOI:10.1007/s10915-008-9232-6.

[5] Erik Burman and Alexandre Ern. A continuous finite element method with face penalty to approximate Friedrichs' systems. *M2AN Math. Model. Numer. Anal.*, 41(1):55–76, 2007.

[6] Erik Burman and Alexandre Ern. Continuous interior penalty *hp*-finite element methods for advection and advection-diffusion equations. *Math. Comp.*, 76(259):1119–1140 (electronic), 2007.

[7] Erik Burman and Miguel A. Fernández. Finite element methods with symmetric stabilization

for the transient convection–diffusion–reaction equation. *Comput. Methods Appl. Mech. Engrg.*, 2009. In press.

[8] B. Cockburn, S. Hou, and C.-W. Shu. The Runge-Kutta local projection discontinuous Galerkin finite element method for conservation laws. IV. The multidimensional case. *Math. Comp.*, 54(190):545–581, 1990.

[9] B. Cockburn, G. E. Karniadakis, and C.-W. Shu. *Discontinuous Galerkin Methods - Theory, Computation and Applications*, volume 11 of *Lecture Notes in Computer Science and Engineering*. Springer, 2000.

[10] B. Cockburn, S. Lin, and C.-W. Shu. TVB Runge-Kutta local projection discontinuous Galerkin finite element method for conservation laws. III. One-dimensional systems. *J. Comput. Phys.*, 84(1):90–113, 1989.

[11] B. Cockburn and C.-W. Shu. TVB Runge-Kutta local projection discontinuous Galerkin finite element method for conservation laws. II. General framework. *Math. Comp.*, 52(186):411–435, 1989.

[12] Ramon Codina. Stabilization of incompressibility and convection through orthogonal sub-scales in finite element methods. *Comput. Methods Appl. Mech. Engrg.*, 190(13-14):1579–1599, 2000.

[13] Ramon Codina. Stabilized finite element approximation of transient incompressible flows using orthogonal subscales. *Comput. Methods Appl. Mech. Engrg.*, 191(39-40):4295–4321, 2002.

[14] Daniele A. Di Pietro, Alexandre Ern, and Jean-Luc Guermond. Discontinuous Galerkin methods for anisotropic semidefinite diffusion with advection. *SIAM J. Numer. Anal.*, 46(2):805–831, 2008.

[15] Jim Douglas, Jr. and Thomas F. Russell. Numerical methods for convection-dominated diffusion problems based on combining the method of characteristics with finite element or finite difference procedures. *SIAM J. Numer. Anal.*, 19(5):871–885, 1982.

[16] A. Ern and J.-L. Guermond. *Theory and Practice of Finite Elements*, volume 159 of *Applied Mathematical Sciences*. Springer-Verlag, New York, NY, 2004.

[17] A. Ern and J.-L. Guermond. Discontinuous Galerkin methods for Friedrichs' systems. I. General theory. *SIAM J. Numer. Anal.*, 44(2):753–778, 2006.

[18] J.-L. Guermond. Stabilization of Galerkin approximations of transport equations by subgrid modeling. *Math. Model. Numer. Anal. (M2AN)*, 33(6):1293–1316, 1999.

[19] J.-L. Guermond. Subgrid stabilization of Galerkin approximations of linear monotone operators. *IMA J. Numer. Anal.*, 21:165–197, 2001.

[20] E. Hairer, S. P. Nørsett, and G. Wanner. *Solving ordinary differential equations. I*, volume 8 of *Springer Series in Computational Mathematics*. Springer-Verlag, Berlin, second edition, 1993. Nonstiff problems.

[21] F. Hecht. *FreeFem++, Third Edition, Version 3.0-1. User's Manual*. LJLL, University Paris VI.

[22] C. Johnson and J. Pitkäranta. An analysis of the discontinuous Galerkin method for a scalar hyperbolic equation. *Math. Comp.*, 46(173):1–26, 1986.

[23] P. Lesaint and P.-A. Raviart. On a finite element method for solving the neutron transport equation. In C. de Boors, editor, *Mathematical aspects of Finite Elements in Partial Differential Equations*, pages 89–123. Academic Press, 1974.

[24] Doron Levy and Eitan Tadmor. From semidiscrete to fully discrete: stability of Runge-Kutta schemes by the energy method. *SIAM Rev.*, 40(1):40–73 (electronic), 1998.

[25] O. Pironneau. On the transport-diffusion algorithm and its applications to the Navier-Stokes equations. *Numer. Math.*, 38(3):309–332, 1981/82.

[26] Hans-Görg Roos, Martin Stynes, and Lutz Tobiska. *Robust numerical methods for singularly perturbed differential equations*, volume 24 of *Springer Series in Computational Mathematics*. Springer-Verlag, Berlin, second edition, 2008. Convection-diffusion-reaction and flow problems.

[27] Qiang Zhang and Chi-Wang Shu. Error estimates to smooth solutions of Runge-Kutta discontinuous Galerkin methods for scalar conservation laws. *SIAM J. Numer. Anal.*, 42(2):641–666 (electronic), 2004.

[28] Qiang Zhang and Chi-Wang Shu. Error estimates to smooth solutions of Runge-Kutta discontinuous Galerkin method for symmetrizable systems of conservation laws. *SIAM J. Numer. Anal.*, 44(4):1703–1720 (electronic), 2006.